Historical Biology
An International Journal of Paleobiology

Taylor & Francis
Taylor & Francis Group

ISSN: 0891-2963 (Print) 1029-2381 (Online) Journal homepage: www.tandfonline.com/journals/ghbi20

A new bird-like dinosaur from the Upper Cretaceous of Mongolia with extremely robust hands supports niche partitioning among velociraptorines

Léa Moutrille, Andrea Cau, Tsogtbaatar Chinzorig, François Escuillié, Khishigjav Tsogtbaatar, Bayasgaa Ganzorig, Christophe Mallet & Pascal Godefroit

To cite this article: Léa Moutrille, Andrea Cau, Tsogtbaatar Chinzorig, François Escuillié, Khishigjav Tsogtbaatar, Bayasgaa Ganzorig, Christophe Mallet & Pascal Godefroit (13 Jul 2025): A new bird-like dinosaur from the Upper Cretaceous of Mongolia with extremely robust hands supports niche partitioning among velociraptorines, Historical Biology, DOI: 10.1080/08912963.2025.2530148

To link to this article: https://doi.org/10.1080/08912963.2025.2530148

HISTORICAL BIOLOGY
https://doi.org/10.1080/08912963.2025.2530148

Taylor & Francis
Taylor & Francis Group

RESEARCH PAPER

A new bird-like dinosaur from the Upper Cretaceous of Mongolia with extremely robust hands supports niche partitioning among velociraptorines

Léa Moutrille[1,2], Andrea Cau[3], Tsogtbaatar Chinzorig[4,5], François Escuillié[6], Khishigjav Tsogtbaatar[5], Bayasgaa Ganzorig[5], Christophe Mallet[7,8] and Pascal Godefroit[8]

[1]University of Poitiers, Poitiers, France; [2]University of Montpellier, Montpellier, France; [3]Unaffiliated, Parma, Italy; [4]North Carolina State University, Raleigh, USA; [5]Institute of Paleontology, Mongolian Academy of Sciences, Ulaanbaatar, Mongolia; [6]Eldonia, Gannat, France; [7]Faculty of Engineering, University of Mons, Department of Geology and Applied Geology, Mons, Belgium; [8]Royal Belgian Institute of Natural Sciences, Brussels, Belgium

ABSTRACT

Dromaeosauridae is a clade of bird-like theropod dinosaurs including, among others, the genera *Deinonychus* and *Velociraptor*, and characterised by a specialised second toe bearing an enlarged and falciform ungual. Here, we describe an exquisitely-preserved velociraptorine dromaeosaurid from the Upper Cretaceous Djadokhta Formation of Mongolia, and refer it to the new species *Shri rapax*. This dromaeosaurid is diagnosed by a peculiar combination of vertebral and pelvic features and by an exceptionally robust hand with a very stout pollex bearing the ungual proportionally larger than in any other dromaeosaurid. Combined with cranial adaptations which could support a bite more powerful than in other velociraptorines, the enlarged unguals in both *Shri* species suggest ecological partitioning in prey preference among the sympatric Djadokhtan dromaeosaurids.

ARTICLE HISTORY
Received 14 April 2025
Accepted 10 July 2025

KEYWORDS
Cretaceous; Djadokhta Formation; Dromaeosauridae; Mongolia; Theropoda

HANDLING EDITOR
Dr Mark Thomas; Young University of Edinburgh

Introduction

Dromaeosauridae is a clade of small- to medium-sized theropod dinosaurs known from several Cretaceous units from North America, Asia, Europe, South America and eventually Antarctica and Madagascar (Norell & Makovicky, 2004; Pittman et al., 2020; Turner et al., 2012). Feather-like integumentary structures, true pennaceous feathers and remnants of the digestive tract are found in exceptionally-preserved dromaeosaurids from the Lower Cretaceous Jehol Biota of north-eastern China (e.g. *Daurlong wangi*, *Sinornithosaurus millenii*, *Microraptor zhaoianus*) (Li et al., 2012; Norell & Xu, 2005; Wang et al., 2022). Along with troodontids, dromaeosaurids are universally considered as the closest relatives of birds among dinosaurs (e.g. Agnolín & Novas, 2013; Burnham et al., 2000; Cau, 2018; Foth et al., 2014; Hartman et al., 2019; Norell & Makovicky, 1997, 1999; Norell & Xu, 2005; Turner et al., 2012). Accordingly, dromaeosaurids are frequently used as models for inferring features of the ancestral body plan of birds (e.g. Norell & Makovicky, 1997, 1999) and as outgroups in phylogenetic analyses focusing on Mesozoic avialans. Yet the assumption that the Cretaceous dromaeosaurids (in particular, the eudromaeosaurs like *Deinonychus antirrhopus* and *Velociraptor mongoliensis*) express the condition ancestral to birds more accurately than other paravian theropods underestimates dromaeosaurid internal diversity (Cau et al., 2017; Turner et al., 2012) and its significant divergence from the ancestral paravian bauplan (Cau, 2018; Pittman et al., 2020).

A rich record of dromaeosaurids from Mongolia and Inner Mongolia (China) is known, which spans the whole Cretaceous (Cau et al., 2017; Pittman et al., 2020; Turner et al., 2021, 2007; Xu et al., 2010). Three taxa have been recorded in pre-Campanian units: the Berriasian-Hauterivian *Shanag ashile* Turner et al., 2007, the Barremian-Aptian *Daurlong wangi* Wang et al., 2022, and the Cenomanian-Santonian *Achillobator giganticus* Perle et al., 1999. Uppermost Cretaceous (Campanian-Maastrichtian) Mongolian dromaeosaurids include *Adasaurus mongoliensis* Barsbold, 1983, from the Nemegt Formation, and several taxa from 'Djadokhta-like' units (lithobiotopes *sensu* Jerzykiewicz et al., 2021; see Dingus et al., 2008; Godefroit et al., 2008). Four dromaeosaurid species come from the Djadokhta Formation: the well-known *Velociraptor mongoliensis* Osborn, 1924, *Tsaagan mangas* Norell et al., 2006, *Mahakala omnogovae* Turneret al., 2007 (see Turner et al., 2011), and

CONTACT Andrea Cau cauand@gmail.com Imbriani M.R. Street, 64, PR 43125, Italy
Supplemental data for this article can be accessed online at https://doi.org/10.1080/08912963.2025.2530148

Published online 13 Jul 2025

Halszkaraptor escuilliei Cau et al., 2017. Two other species, *Velociraptor osmolskae* Godefroit et al., 2008, and *Linheraptor exquisitus* Xu et al., 2010 (see Xing et al., 2015) are known from the Bayan Mandahu Formation of Inner Mongolia, regarded as the Chinese equivalent of the Djadokhta Formation in Mongolia. Finally, the Late Cretaceous Baruungoyot Formation includes several dromaeosaurid species: *Hulsanpes perlei* Osmólska, 1982 (see Cau & Madzia, 2018), *Shri devi* Turner et al., 2021 (see also Czepiński, 2023) and *Kuru kulla* Napoli et al., 2021, all from the Khulsan locality, and *Natovenator polydontus* Lee et al., 2022, from the Hermiin Tsav locality.

Origin of the specimen

The dromaeosaurid specimen herein described was illegally poached before 2010, then retained in private collections in Japan and England before being acquired by the French company Eldonia (Figure 1). The skull and the first four articulated cervical vertebrae were separated from the rest of the material and scanned at the Royal Belgian Institute of Natural Sciences (RBINS) in 2016 before being returned to the owner (Figure 2). At the time of submission of this manuscript, the location of the skull and the first four cervical vertebrae is unknown. Subsequent negotiations between the RBINS, Eldonia and Mongolian authorities, within the scope of the official cooperation agreement between the Ministry of Education, Culture and Science of Mongolia, the Belgian Science Policy Office, and the RBINS, led to the official return of the specimen to the Institute of Paleontology of the Mongolian Academy of Sciences (MPC-D). A cast of the lost material was printed using the scan data obtained in 2016, and included in the material associated to the specimen. The rest of the specimen was only superficially prepared before it arrived at the RBINS, where additional preparation was carried out under the supervision of PG (Figures 3–14). That work has enabled the uncovering of the right arm and the left pelvic bones still inside the matrix (Figures 10, 12), and further preparation of the parts that were already visible. The specimen was then consolidated and assembled coherently. The single femur, initially assembled in one piece, has resulted being a composite from parts of both femora (compare Figures 1 to 13 and 14).

Figure 1. Holotype of *Shri rapax* sp. nov. MPC-D 102/117 in 2010, before preparation at the Royal Belgian Institute of Natural Sciences. The arrow indicates the single femur reconstructed using elements from both femora (elements separated during preparation; see Figure 13 and 14). Scale bar = 40 mm.

Based on the documents associated to the specimen, it is referred to the Djadokhta Formation, and probably from the Ukhaa Tolgod locality (Campanian) like the holotype of *Halszkaraptor escuilliei* (Cau et al., 2017; Dingus et al., 2008). As with MPC-D 102/109 (Cau et al., 2017), the sediment encasing the skeleton is composed of friable reddish-orange sandstone, resembling Facies S ('structureless sandstone lacking concretions or cross-strata' of Dingus et al., 2008) of the Ukhaa Tolgod locality. This sand-slide facies has been interpreted as fluvio-aeolian in origins (Dingus et al., 2008). Many tetrapod skeletons are known from these facies, which are the most fossiliferous of the locality, including oviraptorid and ceratopsian dinosaurs, tiny mammals, and lizards in almost perfect completeness and preservation (Dingus et al., 2008). As we outline in the discussion, the peculiar taphonomy of the specimen further supports its referral to the Djadokhta Formation. However, as with the *Halszkaraptor escuilliei* holotype, it is possible that the specimen may have been found in another 'Djadokhtan' locality than Ukhaa Tolgod, such as in the similar deposits of the Bayn Dzak locality of the Djadokhta Formation in southern Mongolia (Cau et al., 2017).

Material and methods

The description of the skull, mandible and first four cervical vertebrae is based on the photographs, the CT-scan and the cast made before the loss of that material. The skull and first four cervical vertebrae were preliminarily CT-scanned in 2016 at the Gasthuisberg Hospital, Leuven, Belgium, with a Siemens Sensation 64 device. It was scanned helically in the coronal plane with a slice thickness of 1 mm and a 0.5-mm overlap. Data was

Figure 2. Skull of *Shri rapax* sp. nov., MPC-D 102/117. (a-e) cast of the skull and associated first cervical vertebrae in right lateral view (a), dorsal view (b), ventral view (c), left lateral view (d) and posterior view (e). (f) close up of the photograph of the specimen in 2010 before its loss, showing the skull in right lateral view. Abbreviations: a, angular; aof, antorbital fenestra; c3, c4, cervical vertebrae 3 and 4; d, dentary; emf, external mandibular fenestra; f, frontal; itf, infratemporal fenestra; j, jugal; la, lacrimal; mx, maxilla; mxf, maxillary fenestra; na, nasal; or, orbit; p, parietal; pm, premaxilla; po, postorbital; pop, paroccipital process; qj, quadratojugal; sa, surangular; scl, scleral ossicles; sp, splenial; sq, squamosal; stf, supratemporal fenestra. Scale bar = 100 mm (a-e), 50 mm (f).

output in DICOM format and imported into Amira 5.1 or Artecore 1.0-rc3 (Nespos, VisiCore Suite) for viewing and measurement. Since the preliminary CT-scan was not aimed to be used for a detailed, technical analysis, and the missing material was not professionally prepared neither accurately measured before its loss, the anatomical information obtained from the lost skull is limited. Yet, we report all available information to document and certify its original articulation with the rest of the postcranial material, hoping for a future relocation of the material.

Following Articles 72.10F, 73.1.4 and 73B of the Fourth Edition of the International Code of Zoological Nomenclature, the diagnosis of the new species is conservatively based only on the features which can be directly checked on the preserved postcranial skeleton, and does not include elements from the lost cranial and vertebral elements, in order to exclude any spurious feature due to some misinterpretation of the photographs and the scan data of the unprepared material, which could not be falsified without the original specimen.

Photography and 3D model

A complete 3D model of the specimen has been reconstructed using a photogrammetric approach (Mallison & Wings, 2014). We realised 508 pictures of the skeleton (445 on the main face exposing the right side of the specimen, and 63 on the other side exposing mainly the right forelimb). Pictures were realised by T. Hubin, photographer at the RBINS, using a Nikon D850 and a Nikon AF-S DX Micro-NIKKOR 40 mm f2.8 G lens. Pictures were taken at a resolution of 300 dpi, with

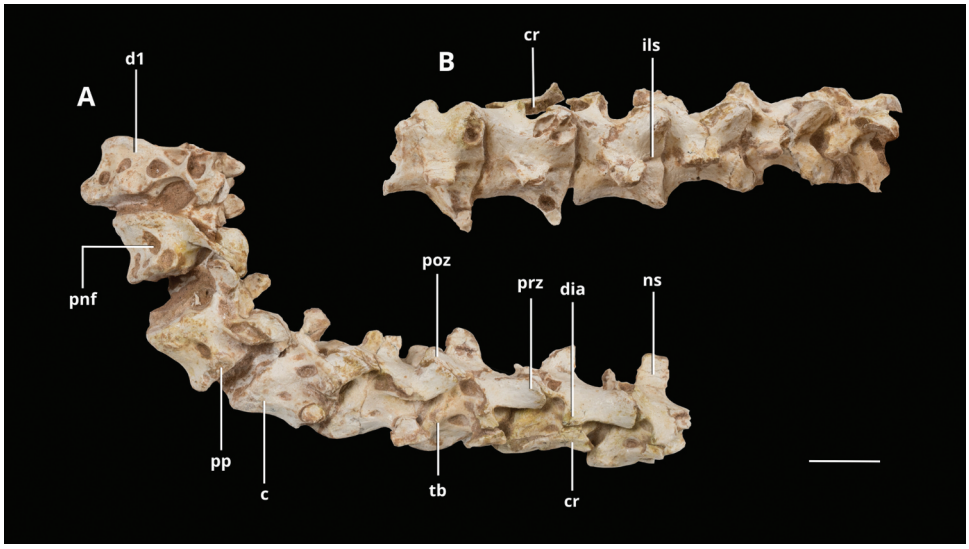

Figure 3. Cervical vertebrae 5 to 11 and first dorsal vertebra of *Shri rapax* sp. nov., MPC-D 102/117 in right lateral view (a) and cervical vertebrae 6 to 11 in dorsal view (b). Abbreviations: c, centrum; cr, cervical rib; d1, first dorsal vertebra; dia, diapophysis; ils, interspinous ligament scar; ns, neural spine; pnf, pneumatic foramen; poz, postzygapophysis; pp, parapophysis; prz, prezygapophysis; tb, tuberosity. Scale bar = 20 mm.

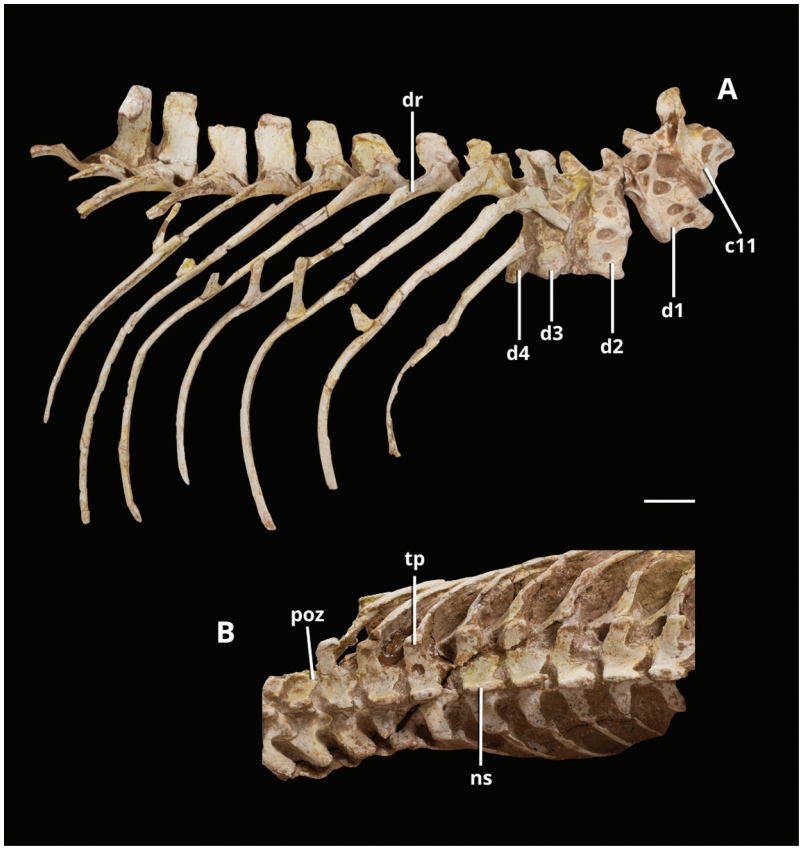

Figure 4. Cervicodorsal vertebrae (a) and dorsal vertebrae (b) of *Shri rapax* sp. nov., MPC-D 102/117 in right lateral view (a) and dorsal view (b). Abbreviations: dr, dorsal rib; c11, eleventh cervical vertebra; d1-d4, dorsal vertebrae 1 to 4; ns, neural spine; poz, postzygapophysis; tp, transverse process. Scale bar = 20 mm.

a focal of 8 and an exposure time of 1/160. We used the software Agisoft Photoscan (v.1.4.3) (Agisoft, 2018) to reconstruct the 3D model using these pictures. After the creation of a dense cloud (in high quality) of 43 million

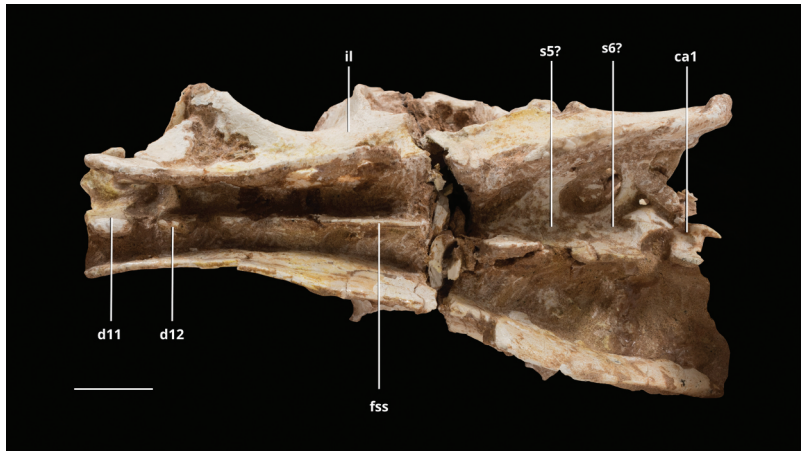

Figure 5. Sacral region of *Shri rapax* sp. nov., MPC-D 102/117 in dorsal view. Abbreviations: ca1, first caudal vertebra; d11-d12, dorsal vertebrae 11 to 12; fss, fused sacral neural spines; il, ilium; s5-s6, sacral vertebrae 5 to 6. Scale bar = 20 mm.

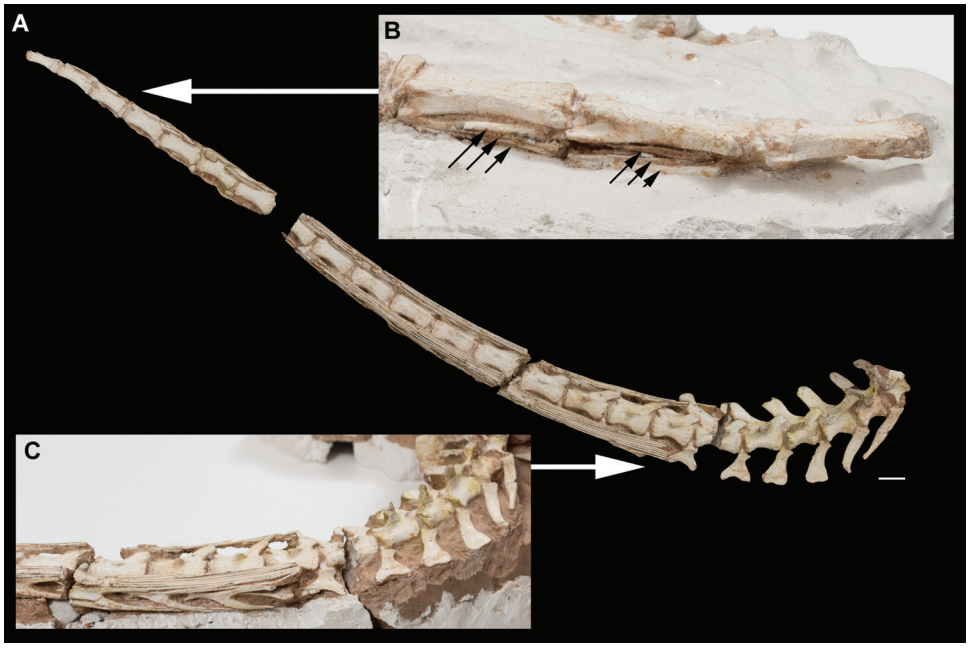

Figure 6. Caudal vertebrae of *Shri rapax* sp. nov., MPC-D 102/117 in right lateral view (a). Close up of the distal end of the tail in dorsal view (b). Close up of the tail in right ventrolateral view showing the cranial end of the caudotheca (c). Arrows in (b) indicate the rod-like extension of the prezygapophyses adjacent to the 21st and 22nd caudal vertebrae. Scale bar in (a) = 20 mm.

points, we created a 3D mesh composed of 5 million faces and a mosaic texture of the complete specimen. This reconstruction was performed on a Lenovo Thinkbook with a 13th Gen Intel Core i9 -13,900 H cpu (2.60 GHz), 32 GB of RAM and a NVIDIA GeForce RTX 4060 Laptop GPU. A series of pictures of the 3D model is included in the Supplementary Material 3 (Supplementary Figures S1-5). The 3D model of the specimen has been uploaded on the Orthanc ecosystem, a free and open-source data management environment initially developed for medical purposes (Jodogne, 2018). The 3D model is stored at doi.https://doi.org/10.6084/m9.figshare.29366354 and can be viewed freely at the following link: https://virtual-collections.naturalsciences.be/3DHOPviewer/shri_rapax.html

Nomenclatural act

The electronic version of this article in Portable Document Format (PDF) will represent a published

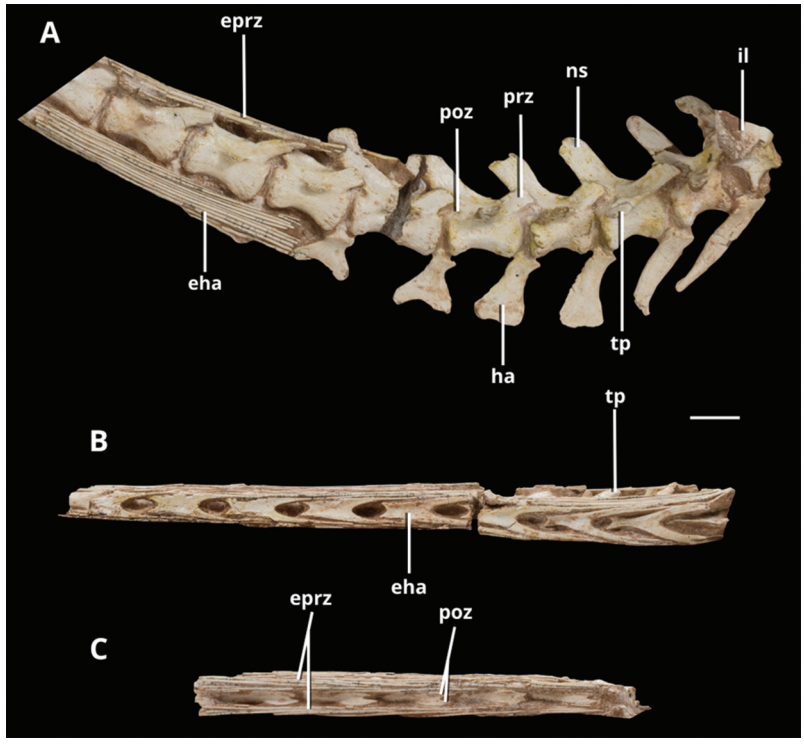

Figure 7. Selected elements in the caudal vertebrae of *Shri rapax* sp. nov. MPC-D 102/117 in right lateral view (a), ventral view (b), and dorsal view (c). Abbreviations: eha, elongate haemal arch; eprz, elongate prezygapophysis; ha, haemal arch; il, ilium; ns, neural spine; poz, postzygapophysis; prz, prezygapophysis; tp, transverse process. Scale bar = 20 mm.

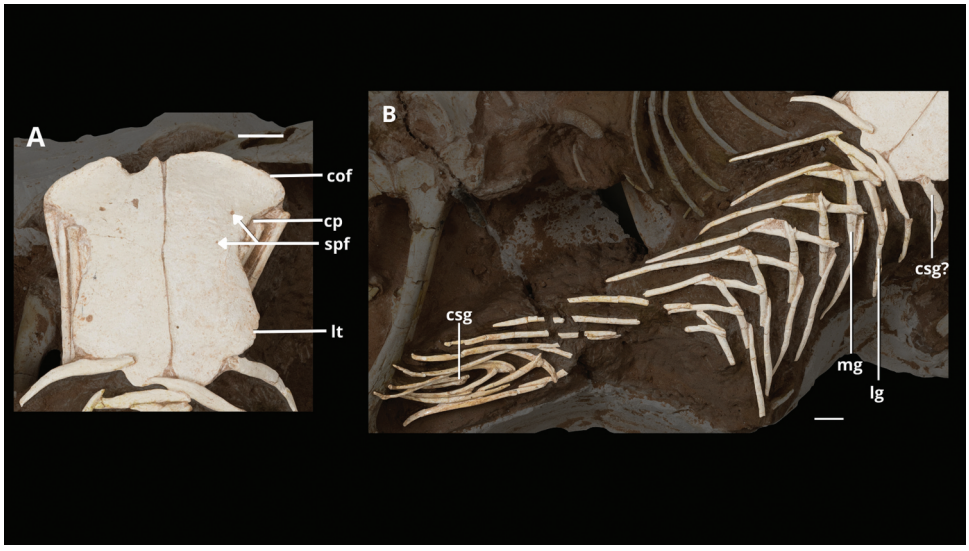

Figure 8. Sternal plates and sternal ribs (a) and gastralia (b) of *Shri rapax* sp. nov. MPC-D 102/117 in ventral view. Abbreviations: cof, coracoid facet; cp, costal process; csg, chevron-shaped gastralium; lg, lateral gastralium; lt, lateral trabecula; mg, medial gastralium; spf, sternal plate foramina. Scale bar = 20 mm.

work according to the International Commission on Zoological Nomenclature (ICZN), and hence the new names contained in the electronic version are effectively published under that Code from the electronic edition alone. This published work and the nomenclatural acts it contains have been registered in ZooBank, the online registration system for the ICZN. The ZooBank LSIDs (Life Science Identifiers) can be resolved and the associated information viewed through any standard web browser by appending the LSID to the prefix http://zoobank.org/. The LSID for this publication is: LSIDurn:lsid:

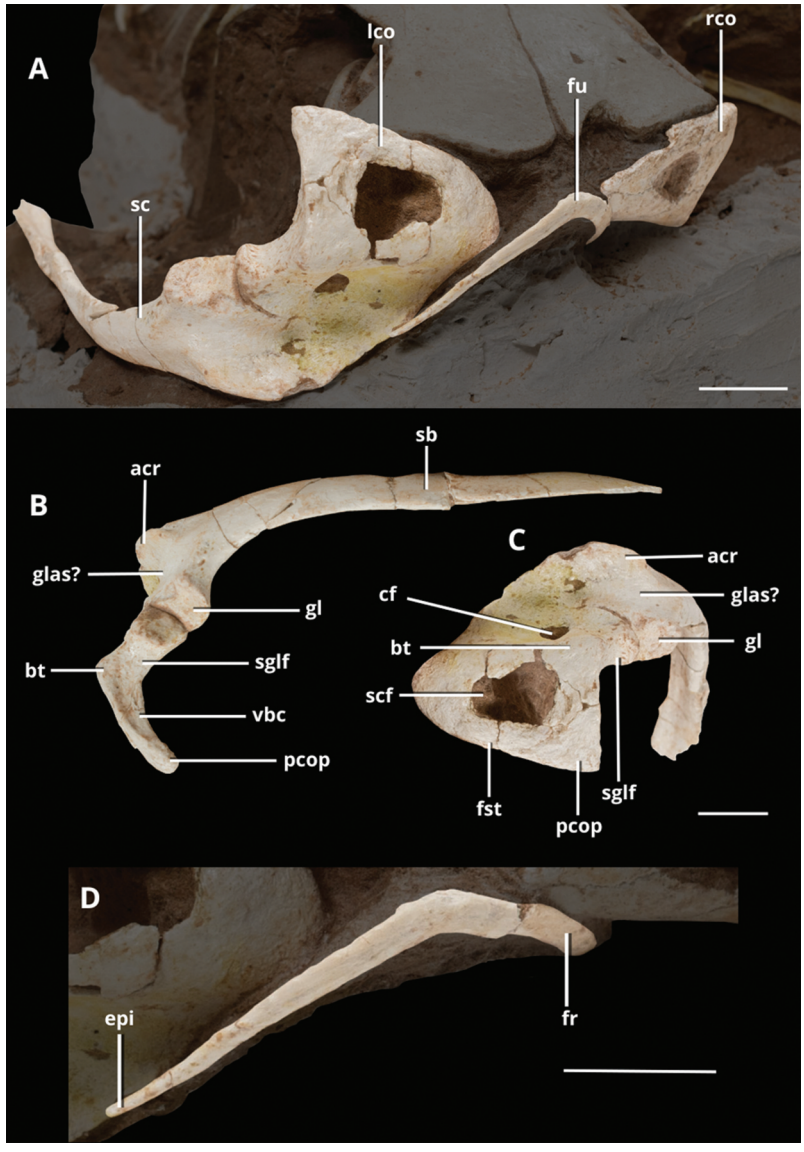

Figure 9. Scapulocoracoid and furcula of *Shri rapax* sp. nov., MPC-D 102/117. (a) articulated elements in anteroventral view. Left scapulocoracoid in lateral view (b) and anterior view (c). Detail of articulated furcula in anteroventral view (d). In (a) and (d), ventral surface above. Abbreviations: acr, acromion; bt, 'bicipital' tuber; cf, coracoid foramen; epi, epicleidium; fr, furcular ramus; fst, facet for sternum; fu, furcula; gl, glenoid; glas, glenohumeral ligament attachment site; lco, left coracoid; pcop, posterior coracoid process; rco, right coracoid; sb, scapular blade; sc, scapula; scf, supracoracoid fenestra; sglf, subglenoid fossa; vbc, ventral blade of coracoid. Scale bar = 20 mm.

zoobank.org:pub:E4F72D4C-23FC-4158–8901-F9FE4910E642. The online version of this work is archived and available from the following digital repositories: PeerJ, PubMed Central SCIE and CLOCKSS.

The LSID for the new species (*Shri rapax*) is: LSIDurn:lsid:zoobank.org:act:E3C7FC28-4E32-448F-AE20-8F73E6530C4A

Phylogenetic analysis

The new theropod is unambiguously referrable to Dromaeosauridae based on several derived features in the skull, vertebrae and appendicular skeleton (e.g. the presence of the caudotheca, Senter et al., 2012; see Discussion). In order to test its particular affinities among dromaeosaurids, we included it in a phylogenetic matrix focusing on that clade. The data set is based on the theropod phylogenetic analysis of Cau (2024) retaining only the dromaeosaurid taxa recovered in the original analysis (Supplementary Material 2 and 3). The Jurassic coelurosaurs *Guanlong wucaii*, *Ornitholestes hermanni*, *Aurornis xui* and *Archaeopteryx lithographica* have been used as outgroups. The dataset was analysed using equally weighted parsimony in TNT 1.6 (Goloboff &

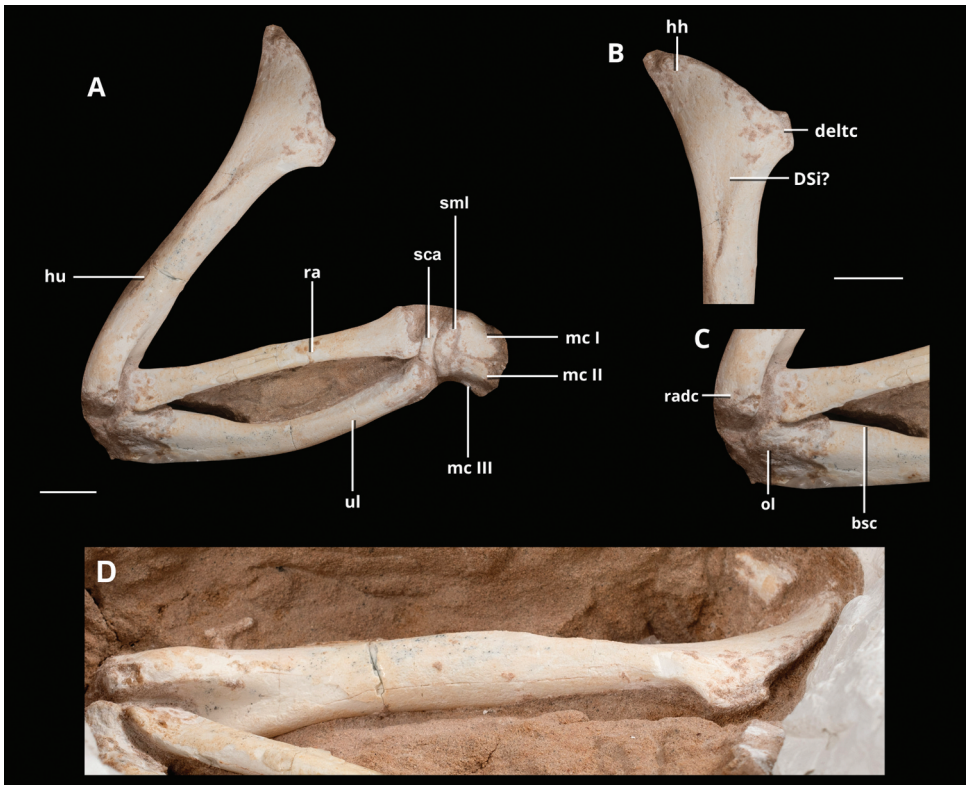

Figure 10. Right forelimb of *Shri rapax* sp. nov., MPC-D 102/117 in right lateral view (a). Enlarged on: proximal end of the humerus (b); distal end of humerus and proximal ends of radius and ulna (c); (d) humerus in cranial view. Abbreviations: bsc, bicipital scar; deltc, deltopectoral crest; DSi, insertion for the *M. deltoides scapularis*; hh, humeral head; hu, humerus; mcI-III, proximal end of metacarpal I to III; ol, olecranon; ra, radius; radc, radial condyle; sca, scapholunare; sml, semilunate; ul, ulna. Scale bar = 20 mm.

Figure 11. Right manus of *Shri rapax* sp. nov. MPC-D 102/117 in distoventral view. Abbreviations: mcI-III, metacarpal I to III; px, phalanx. Scale bar = 20 mm. Note that phalanx II-3 is reconstructed.

Morales, 2023). All analyses were performed setting maxtree = 50.000. We performed 1000 'Traditional search' runs using default settings, then explored the tree islands stored in the RAM during the first search round. Nodal support was calculated replicating the analysis and saving all trees up to 10 steps longer than the shortest topologies. Dromaeosaurid nomenclature follows Cau et al. (2017).

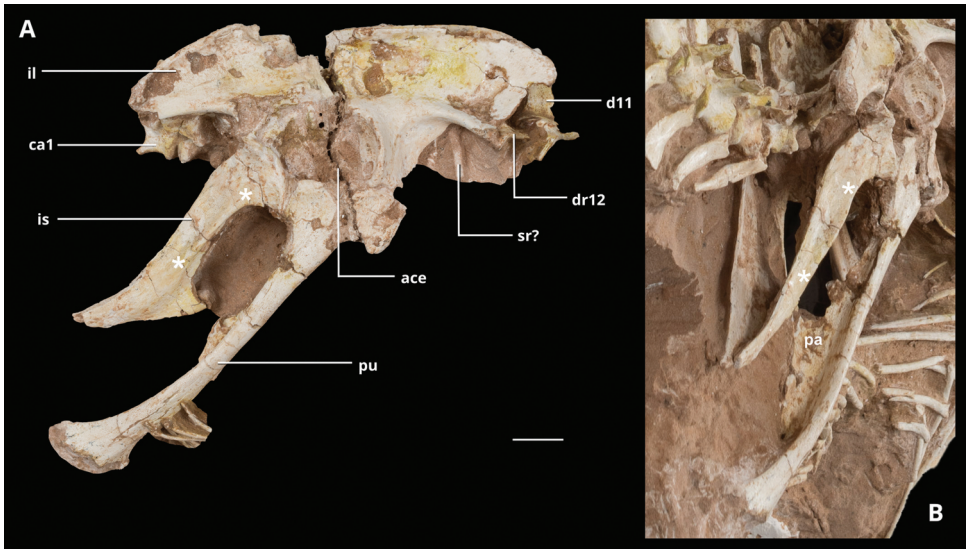

Figure 12. Pelvis of *Shri rapax* sp. nov., MPC-D 102/117 in right lateral view (a) and right posteroventral view (b). Abbreviations: ace, acetabulum; ca1, first caudal vertebra; d11–12, dorsal vertebrae 11 and 12; il, ilium; is, ischium; pa, pubic apron; pu, pubis; ?sr, possible fragment of sternal rib. The asterisks indicate the extent of the lateral shelf of the ischium. Scale bar = 20 mm.

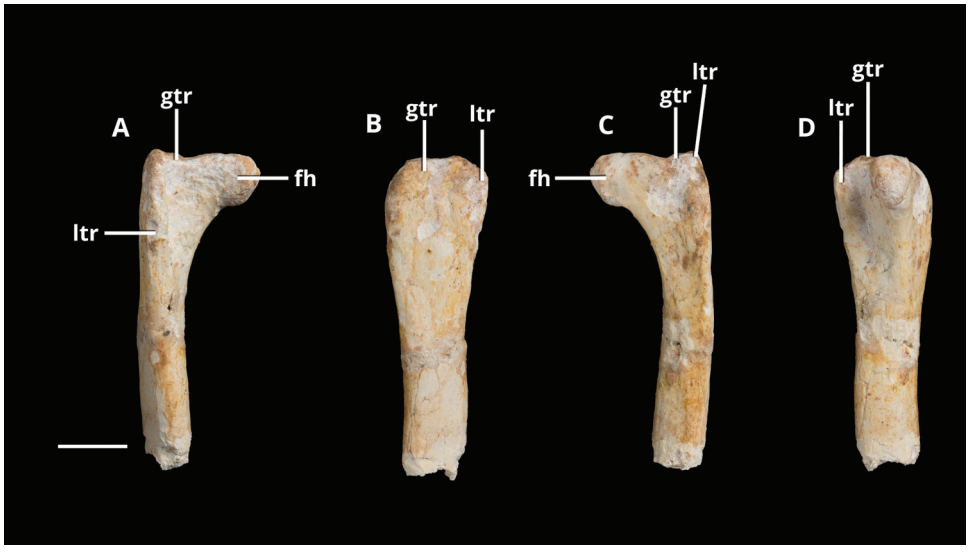

Figure 13. Proximal end of the right femur of *Shri rapax* sp. nov., MPC-D 102/117 in cranial (a), lateral (b), caudal (c) and medial (d) view. Abbreviations: fh, femoral head; gtr, greater trochanter; ltr, lesser trochanter. Scale bar = 20 mm.

Morphometric analysis

We compared the relative elongation of the caudal vertebrae in the new specimen with a sample of dromaeosaurid and non-dromaeosaurid theropod caudal series. The caudal series were normalised dividing the length of each caudal centrum to the sum of the lengths of caudal centra 6th, 7th and 8th in each series (the only elements which are consistently preserved in all sampled specimens; Supplementary Material 3). We performed a Principal Component Analysis of the normalised ratios along caudal centra 6th to 23rd (the distalmost preserved vertebra in the new specimen) in PAST vers. 4.04 (Hammer et al., 2001), using 1000 iterative imputations for the missing entries.

Institutional abbreviations: AMNH, American Museum of Natural History, New York; IVPP, Institute of Vertebrate Paleontology and Paleoanthropology, Beijing; MPC-D, Institute of Paleontology of the Mongolian Academy of Sciences, Ulaanbaatar.

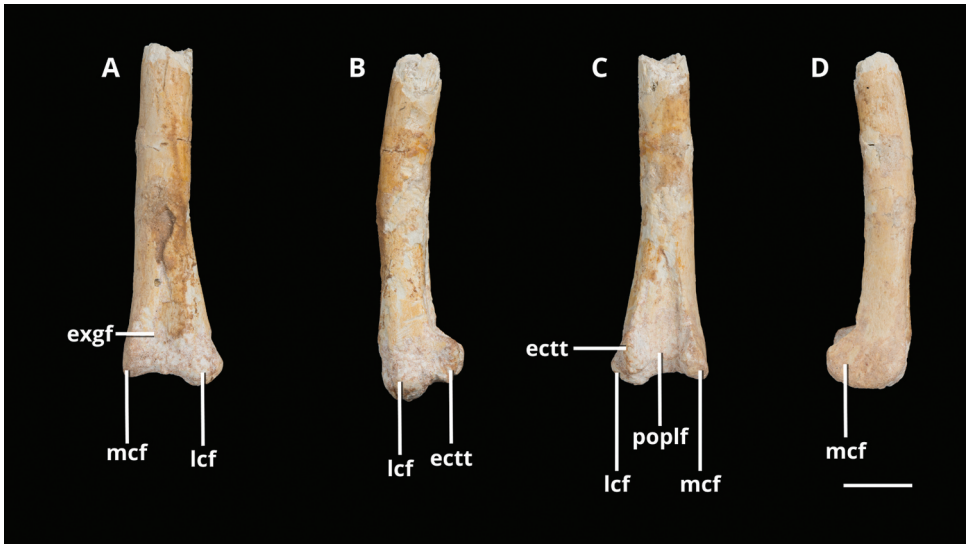

Figure 14. Distal end of the left femur of *Shri rapax* sp. nov., MPC-D 102/117 in cranial (A), lateral (B), caudal (C) and medial (D) view. Abbreviations: ectt, ectocondylar tuber; exgf, extensor fossa; lcf, lateral femoral condyle; mcf, medial femoral condyle; poplf, popliteal fossa. Scale bar = 20 mm.

Systematic paleontology

Dinosauria Owen, 1842
Theropoda Marsh, 1881
Maniraptora Gauthier, 1986
Dromaeosauridae Matthew & Barnum Brown, 1922
Velociraptorinae Barsbold, 1983
Shri Turner et al., 2021

Shri rapax sp. nov.

Holotype. MPC-D 102/117 (Figures 1–14; measurements in Supplementary Material 1). An almost complete and articulated skeleton: almost complete skull (now lost), vertebral series with associated ribs (first four cervical vertebrae now lost); both sternal plates; complete gastral series; left scapula; right and left coracoid; furcula; gastralia; complete right forelimb and manus; complete pelvis; proximal section of the right femur and distal section of the left femur.

Etymology. From Latin, *rapax*, 'rapacious': the term refers to the hypertrophied falciform pollex ungual present in this species.

Type locality and horizon. The exact locality of the specimen is unknown. Based on the documentation associated with the specimen, we tentatively refer it to Ukhaa Tolgod, Mongolia (see discussion). Djadokhta Formation (Campanian, Upper Cretaceous).

Diagnosis. The specimen can be referred to the genus *Shri* (Czepiński, 2023; Turner et al., 2021) based on the following features: a short antorbital fenestra with nearly equal rostrocaudal and dorsoventral dimensions, where the ventral margin slopes sharply rostrodorsally; angular posterior margin of the maxillary fenestra; the last maxillary tooth located posterior to the rostral end of the maxillo-jugal suture; a 'Z'-shaped maxilla-jugal suture; tuber on the lateral surface of the centra of at least some mid-cervical vertebrae; a secondary pleurocoel on d1 and d2, placed ventrally to the main pleurocoel; medial antiliac shelf of ilium reduced or absent. The new species, *Shri rapax*, is diagnosed by (unambiguous autapomorphies relative to *Shri devi* marked by asterisk): 11 cervical vertebrae; middle cervical centra subequal in length (in *Shri devi*, the fifth cervical centrum is 125% longer than the sixth)*; 7th cervical centrum with tuberosity centred on the lateral surface and placed caudal to the pleurocoel (Figure 3A; in *Shri devi*, tuberosity present in more cervical vertebrae, and placed adjacent to the cranial intercentral facet)*; accessory pleurocoel in last cervical centrum (absent in *Shri devi*)*; infraprezygapophyseal and infradiapophyseal fossae in last cervical neural arch merged into single large fusiform fossa (in *Shri devi*, fossae smaller and widely distinct)*; epipophyses not extended onto the dorsal vertebrae (in *Shri devi*, the epipophyses extend onto the anteriormost dorsal vertebrae)*; deep triangular fossa ventral to the infradiapophyseal and infraprezygapophyseal fossae in dorsal neural arches 1 and 2 (fossa absent in *Shri devi*)*; the accessory ventral

pleurocoel in the anterior dorsal central 1 and 2 is a large opening (in *Shri devi*, it is a smaller opening)*; the accessory pleurocoel in the first dorsal centrum is anteroventral to the main pleurocoel (in *Shri devi*, it is ventral to mid-point of main pleurocoel)*; anterior dorsal hypapophyses more prominent than in *Shri devi* and curved anteriorly*; middle to distal caudal vertebrae proportionally less elongate than in *Deinonychus* and *Velociraptor*; deltopectoral crest low and trapezoidal in lateral view; first metacarpal and first finger very robust, much broader than combined second and third manual digits (unique among paravians); large falciform manual ungual 1, being along dorsal margin more than 160% longer than manual phalanx 1-I (unique among paravians); pubis forming a 135° angle with the long axis of the ilium (pubis forming a 155–160° angle in *Shri devi* and *Velociraptor mongoliensis*); in lateral view, ischium diverging from pubis distal to obturator notch (bones subparallel in *Shri devi*); ischium elongate, 66% of pubis length (about 50% in *Shri devi*); absence of ischial tuber distal to pubic peduncle (present in *Shri devi*); sharp lateral shelf on ischium bound dorsally by a longitudinal depression (as in *V. mongoliensis*; lateral ridge more rounded and depression absent in *Shri devi*); ischium with obturator process extending less than half the length of the ischium (extended for two-thirds the length of the ischium in *Shri devi*) and with sigmoid posterior margin in lateral view (margin straight in *Shri devi*); femur with distal extensor sulcus (sulcus absent in *Shri devi*).

Results

Anatomical description

Skull

The preserved skull measures 178.1 mm and does not include the rostral part of the premaxilla: we estimate the whole skull could be around 200 mm long (Figure 2). The occipital region and the left side of the skull are still mostly covered by sediment and could not be adequately described. In right lateral view, the skull lacks significant deformation (see Czepiński, 2023). The rostrum preserves the maxilla and a small dorsal part of the premaxilla. The snout is estimated to occupy at least 48% of the skull length. The maxilla is shorter and more robust than *Tsaagan mangas* and *Velociraptor mongoliensis* but similar to *Deinonychus antirrhopus*, *Bambiraptor feinbergi* and *Shri devi* (Barsbold & Osmólska, 1999; Burnham et al., 2000; Czepiński, 2023; Norell et al., 2006; Ostrom, 1969; Powers et al., 2021). The antorbital fossa extends approximately across two-thirds of the maxilla, like in most dromaeosaurids (Norell & Makovicky, 2004; Powers et al., 2021). The dorsal ramus of the maxilla is short, similar to the condition in *Bambiraptor feinbergi* and *Achillobator giganticus* (Norell et al., 2006; Powers et al., 2021). The antorbital fenestra length is 93% of its height, which is an even lower proportion than in *Shri devi* (i.e. ratio = 106%; Czepiński, 2023), contrasting with the rostro-caudal elongation of other Djadokhtan dromaeosaurids such as *Velociraptor mongoliensis*, *Tsaagan mangas* and the halszkaraptorines (i.e. ratio range = 129–166%, Barsbold & Osmólska, 1999; Cau et al., 2017; Czepiński, 2023; Norell et al., 2006; Powers et al., 2021). The antorbital fenestra higher than long or equal in height and length is similar to *Saurornitholestes langstoni* and *Sinornithosaurus millenii* (Currie & Evans, 2020; Xu & Wu, 2001). The ventral margin of the antorbital fenestra is oriented rostro-dorsally with an angle of 25° to the dental row, similar to the angle observed in *Shri devi*, *Bambiraptor feinbergi* and *Achillobator giganticus* (Burnham et al., 2000; Currie & Varrichio, 2004; Czepiński, 2023). The maxillary fenestra is located at the mid-line between the rostral border of the antorbital fenestra and the rostral end of the antorbital fossa. The fenestra is lozange-shaped, a condition which could also be present in *Shri devi* (Czepiński, 2023). A small promaxillary fenestra seems to be present, at the level of midline of the maxillary fenestra and delimited by the rostral border of the antorbital fossa. The ventral part of the maxilla, below the antorbital fossa, is low as in *Shri devi* and *Velociraptor mongoliensis* (Barsbold & Osmólska, 1999; Czepiński, 2023) and tapers caudally. It bears a single row of supralabial foramina. The jugal ramus of the maxilla in *Shri rapax* does not reach the level of the lacrimal bar, differing from *Saurornitholestes langstoni*, *Shri devi*, *Tsaagan mangas* and *Velociraptor mongoliensis* (Barsbold & Osmólska, 1999; Currie & Evans, 2020; Czepiński, 2023; Norell et al., 2006). The suture with the jugal is 'Z'-shaped like in *Shri devi*, *Atrociraptor marshalli* and *Saurornitholestes langstoni*, but unlike *Velociraptor mongoliensis*, *Linheraptor exquisitus* and *Tsaagan mangas*, in which there is only a simple suture (Barsbold & Osmólska, 1999; Currie & Evans, 2020; Czepiński, 2023; Norell et al., 2006; Powers et al., 2021; Xu et al., 2010). The nasal is partially visible in the dorsal surface of the cast. The snout is transversely compressed, with subparallel maxillae, as in other velociraptorines (e.g. Barsbold & Osmólska, 1999). A potentially unique feature of *Shri rapax* among velociraptorines is the position of

the lacrimal facet of the jugal relative to the maxillary contact: in the photographs and in both lateral sides of the cast of the skull, the lacrimal facet is steeply raised dorsally, resulting in a distinctly concave jugal margin of the antorbital fenestra. Yet, we cannot exclude that this feature is an artefact due to the presence of encrusting sediment still present when both cast and photographs were made. In other velociraptorines, the lacrimal facet and maxillary contact are aligned along the line linking the ventral margins of the orbital and antorbital fenestrae (Norell et al., 2006; Turner et al., 2012; Xu et al., 2010). The preserved part of the maxilla bears 9 (10?) teeth (the penultimate one is broken). The third rostral tooth is smaller than the two adjacent teeth, maybe because not fully erupted at time of death. The caudal most teeth are smaller than the rostral ones. Like in *Shri devi*, the last maxillary tooth is almost at the same level than the caudal margin of the antorbital fenestra, more posteriorly placed than in other Djadokhtan eudromaeosaurs (Czepiński, 2023). In dorsal view, the cast shows that the lacrimal bears a caudal process extended posterodorsally to the ventral ramus, like all dromaeosaurids (Norell & Makovicky, 2004). The rostral ramus of the lacrimal seems to contact the maxilla and extends along the posterior half of the dorsal border of the antorbital fossa. The end of the lacrimal caudal ramus is not well visible so it is difficult to appreciate its length. The ventral ramus of the lacrimal contacts the jugal and its slightly oriented caudally. There is no evidence of the prefrontal, as in most dromaeosaurids except *Deinonychus antirrhopus* and *Sinornithosaurus millenii* (Maxwell & Witmer, 1996; Xu & Wu, 2001), although this could be an artefact of the cast. Only the rostral part of the right jugal is visible, whereas most of the postorbital ramus is visible in the left element. Caudally, the jugal participates to the half of the postorbital bar. The jugal is inserted into the maxilla by the 'Z'-shaped suture, the ventral process being more robust than the one just below the antorbital fenestra. The caudal border forms the rostral border of the infratemporal fenestra. The orbital margin of the jugal is straight, differing from the more concave margin of *Shri devi* (Czepiński, 2023). The postorbital is triangular and tapers caudally, and largely contacts with the squamosal. The latter is large and forms a major part of the dorsal border of the infratemporal fenestra. That fenestra is much smaller than the orbit, as in other dromaeosaurids (Barsbold & Osmólska, 1999; Cau et al., 2017). The supratemporal fenestra is subcircular in dorsal view, similar to *Velociraptor mongoliensis* (Barsbold & Osmólska, 1999). The cast shows the presence of a sagittal crest along the dorsal surface of the parietal, yet we cannot determine its depth and extent. Only the caudoventral margin of the quadratojugal is visible. The scleral ossicles are preserved in the orbit. In the badly exposed occipital surface, the paroccipital process of the exoccipital does not curve ventrally, differing from the pendant condition of some dromaeosaurids (e.g. *Mahakala omnogovae*, Turner et al., 2011).

Mandible. The dentary lacks its rostral-most part. It is low with subparallels ventral and dorsal margins like in *Tsaagan mangas* and *Shri devi* (Czepiński, 2023; Norell et al., 2006), even if its ventral margin is slightly convex at the contact with the splenial. A row of neurovascular foramina is present parallel to the dorsal margin. Another row of foramina is visible along the ventral margin, similar to *Shri devi* and other velociraptorines except *Kuru kulla* (Czepiński, 2023; Napoli et al., 2021; Norell et al., 2006). Its ventral ramus in contact with the angular is tapered. Only one tooth is observable. The splenial is well exposed in lateral view, as in other eudromaeosaurs. The caudal ramus in contact with the angular is directed caudoventrally, similar to *Shri devi* (Czepiński, 2023). The surangular contacts the dentary rostrally, forming the ventral border of the external mandibular fenestra. Above the external mandibular fenestra, the surangular contacts the dentary rostrally to encloses this fenestra. It approaches the quadratojugal caudally.

Cervical vertebrae

The vertebral series is almost completely preserved and fully articulated, making it among the best preserved in a dromaeosaurid (Figures 2–4). The four rostral-most cervical vertebrae including the atlas and axis are in the block containing the skull, and seven vertebrae are preserved on the post-cranial block (Figure 3). The presence of 11 cervical vertebrae differs from the condition in *Velociraptor mongoliensis* and *Linheraptor exquisitus* (9–10 cervical vertebrae) (Norell & Makovicky, 2004; Xu et al., 2010). Turner et al. (2021) stated that *Shri devi* bears 10 cervical vertebrae, yet, the holotype series is incomplete (missing the first elements), thus we cannot exclude that the latter species shared with *Shri rapax* an additional eleventh cervical vertebra. Yet, when the vertebral series of the two *Shri* species are compared starting from the cervico-dorsal transition frontward, they differ from each other in the pneumatization pattern and in the proportions of the middle centra (see diagnosis), dismissing the hypothesis that their differences

are due to erroneous identification of the cervical count. All the vertebrae are articulated, and connected to the first dorsal vertebra. These are well-preserved, and show no signs of scavenging, a taphonomic condition unlike most dromaeosaurid specimens from the Nemegt Group (e.g. Norell et al., 2006; Turner et al., 2021) but similar to *Halszkaraptor escuilliei* holotype (Cau et al., 2017). The cervical centra are platycoelous with the caudal concavity deeper than the cranial one, like in *Shri devi* and other dromaeosaurids (Norell & Makovicky, 2004; Turner et al., 2021). Like in most dromaeosaurids (Norell & Makovicky, 1997, 1999; Turner et al., 2021), the neural arches make the greatest contribution to the articulation between vertebrae, while the centrum plays a minor role. In dorsal view (Figure 3B), the rostral-most postzygapophyses are directed laterally and become more medially oriented caudally: the cervical vertebrae are more quadrangular cranially and become more 'X'-shaped caudally, as usual among maniraptorans (Makovicky & Sues, 1998). The cranial articular surfaces of cervical centra 5–8 are directed cranioventrally as in *Deinonychus antirrhopus*, *Tsaagan mangas* and *Shri devi* (Norell et al., 2006; Ostrom, 1969; Senter et al., 2004; Turner et al., 2021), whereas their caudal articular surfaces are directed caudodorsally. In lateral view, the caudal articular surface is higher than the cranial one and the angle formed by both articular surfaces (about 60–70° related to the craniocaudal axis) is similar to *Deinonychus antirrhopus* (40° to 75°; Ostrom, 1969). From cervical 9, both articular surfaces progressively become vertical in lateral view, and the ventral margin of the centrum becomes slightly concave. As can be seen on cervical 5, the cranial articular surface of the centrum is distinctly concave, like in *Shri devi* (Turner et al., 2021). In ventral view, the centra are proportionally short and constricted, with the caudal articular surface wider than the cranial one. The centrum is cranio-caudally shorter than the corresponding neural arch, so that the neural arch overlaps the centrum of the preceding vertebra, as in most dromaeosaurids (Cau et al., 2017; Turner et al., 2012). Cervicals 9–11 bear a cranial lip that becomes more raised along the series like in *Velociraptor mongoliensis*, *Saurornitholestes langstoni*, *Tsaagan mangas* and *Shri devi* (Turner et al., 2021). The parapophyses are oval and cranio-laterally directed in cervical 5–8 and more rounded in the succeeding cervicals, like in *Shri devi* (Turner et al., 2021). In the cranial-most vertebrae, they are located on the cranial part of the lateral side of the centra, but they stick to the cranial edge of the centra on the more caudal vertebrae. A pneumatophore is present on the centra on each vertebra, right behind the parapophysis, similar in its location to *Deinonychus antirrhopus* (Ostrom, 1969). An accessory pleurocoel placed dorsal to the main pneumatic foramen is present in the last cervical vertebra, as in the single known posterior cervical vertebra of *Luanchuanraptor henanensis* but not in *Shri devi* (Lü et al., 2007; Turner et al., 2021). Yet, in *Luanchuanraptor henanensis* the accessory foramen is much smaller than in *Shri rapax* (Lü et al., 2007). A small tuberosity is present, just caudal to the pneumatophore, only on cervical 7, differing from *Shri devi* which shows a tuber in several cervical centra but in a more cranial position (Turner et al., 2021). Only cervical 5 is visible in cranial view. Like in *Shri devi*, the neural canal is quadrangular, a little wider than high. The diapophyses are mediolaterally flattened and oriented ventrally, extending up to almost the middle of the centrum, resembling the condition in *Deinonychus antirrhopus*, *Tsaagan mangas, Austroraptor cabazai*, *Buitreraptor gonzalezorum* and *Shri devi* (Gianechini et al., 2018; Norell et al., 2006; Novas et al., 2009; Ostrom, 1969; Turner et al., 2021). From cervical 9, they progressively orient laterodorsally. The prezygapophyses are oval and extend more cranially than the centrum. In most cervical vertebrae, their articular facet is craniomedially oriented, as in *Deinonychus antirrhopus*, *Velociraptor mongoliensis*, *Tsaagan mangas* or *Shri devi* (Ostrom, 1969; Turner et al., 2021). From cervical 8, they progressively orient dorsomedially. In dorsal view, the postzygapophyses are projected laterally (Figure 3B). In cervicals 5 to 6, the postzygapophyses do not extend as far as the caudal end of the centrum, whereas they progressively extend further caudally from cervical 7. Following the general trend observed on the prezygapophyses, the articular facets of the postzygapophyses progressively orient lateroventrally along the cervical series. Above the caudal end of the postzygapophyses, a small epipophysis extends dorsolaterally; on cervicals 5 to 7, it is less developed than in *Deinonychus antirrhopus* (Ostrom, 1969), more closely resembling the condition in *Shri devi* (Turner et al., 2021). The neural spines are parallel to the dorsoventral axis of the vertebra like in *Shri devi* (Turner et al., 2021), whereas on the most cranial vertebrae of *Deinonychus antirrhopus* they project caudally (Ostrom, 1969). The scars for interspinous ligaments are present, cranially and caudally to each neural spine as in *Deinonychus antirrhopus* (Ostrom, 1969). The cervical ribs are at least partly preserved on cervicals 5 to 9. Cranially, the capitulum and the tuberculum are close together; the shaft of the tuberculum then extends dorsally along the vertebrae series. The shaft of the rib tapers caudally and is slightly oriented laterally.

Dorsal vertebrae

There are 12 articulated dorsal vertebrae associated with almost all paired ribs (Figure 4). All centra seem to be amphiplatyan. The complete series is only visible in dorsal view except for the first four dorsals, exposed in right lateral view. The cranial dorsals look slightly shorter than the caudal ones. The last two dorsals are partially covered by the pre-acetabular blade of the ilium. The hypapophyses of dorsals 1 to 2 and 4 are more prominent and cranially curved than in *Shri devi* (Turner et al., 2021). It is probable that dorsal 3 also shares this morphology, but it cannot be observed. The centra bear pleurocoels on their lateral surface, at the junction with the neural arch, like in *Deinonychus antirrhopus* (Ostrom, 1969). On dorsals 1 and 2, one additional pleurocoel is present, just ventrally to the main one (Figure 4), a derived feature shared with *Shri devi* (Turner et al., 2021), *Luanchuanraptor henanensis* (Lü et al., 2007), and an isolated cervicodorsal vertebra from the Upper Cretaceous of France referred to *Variraptor mechinorum* by Le Loeuff and Buffetaut (1998). The accessory pneumatization in the cervicodorsal vertebrae of MPC-D 102/117 differs from *Luanchuanraptor henanensis* and *Shri devi* in the proportions of the accessory pleurocoel relative to the main pleurocoel: in MPC-D 102/117, it is proportionally much larger, being comparable in size to the main pneumatic opening (Lü et al., 2007; Turner et al., 2012). In the French cervicodorsal vertebra referred to *Variraptor mechinorum*, both pleurocentral foramina are proportionally smaller than in MPC-D 102/117 (see Figure 6 in Le Loeuff & Buffetaut, 1998). Furthermore, the first dorsal of *Shri rapax* differs from the the first two dorsal vertebrae of *Shri devi* and the French cervicodorsal in having the accessory pleurocoel placed anteroventrally relative to the main pleurocoel, adjacent to the hypapophysis instead of being strictly ventral to the mid-point of the main pneumatic foramen. The same condition of *Shri rapax* d1 is reported in the known cervicodorsal vertebra of *Luanchanraptor henanensis* (Lü et al., 2007). Multiple pneumatic openings are variably developed in the presacral centra of many dromaeosaurids. The cervicodorsal centra of *Bambiraptor feinbergi* bear multiple pneumatic openings, and a similar condition is reported in the dorsal vertebrae of *Achillobator giganticus* and *Saurornitholestes langstoni* (Burnham, 2004; Perle et al., 1999; Sues, 1978). The presence of two pleurocoels aligned anteroposteriorly in the same vertebra and the presence of a single pneumatic opening subdivided into two foramina by a subvertical septum are usually described as distinct features (e.g. Burnham, 2004; Sues, 1978; Turner et al., 2021). Yet, the two features could co-occur along the same vertebral series, or even be expressed, alternatively, on the two sides of the same vertebra (e.g. *Unenlagia comahuensis*, Novas et al., 2021). We consider the peculiar dorsoventral alignment of two pleurocoels as non-homologous to the craniocaudally aligned foramina, because the former feature is restricted uniquely to the cervicodorsal region and is not expressed along the rest of the presacral series. On dorsals 1 to 2, the prezygapophyses of MPC-D 102/117 are craniomedially oriented and become dorsally oriented from dorsal 3. They reach the same level as the dorsal surface of the neural arch. Caudally, they become almost indistinguishable. The postzygapophyses are oval, with their articular facets directed ventrally, and without epipophyses, unlike *Deinonychus antirrhopus, Luanchuanraptor henanensis* and *Shri devi* (Lü et al., 2007; Ostrom, 1969; Turner et al., 2021). In *Shri devi*, the first dorsal epipophysis is apomorphically prominent (Turner et al., 2021). On dorsals 1 and 2, the transverse processes are long and thin, with thickened lateral ends like in other dromaeosaurids (Norell & Makovicky, 1999). These extremities are slightly curved caudally. The neural spines are high and flat, with more rounded and rugose dorsal margins. A deep pneumatic opening, named hapidocoel by Ostrom (1969) can be observed on dorsals 1 and 2, at the base of the prezygapophysis and transverse process. This structure is also present in *Deinonychus antirrhopus*, *Luanchuanraptor henanensis* and *Shri devi* (Lü et al., 2007; Ostrom, 1969; Turner et al., 2021) and considered by Turner et al. (2021) as homologous of the infraprezygapophyseal fossa on the succeeding vertebrae. Another deep fossa is located on the lateral side of the neural arches of dorsals 1 and 2. It is bordered cranially by the prezygoparapophyseal lamina, caudodorsally by the prezygodiapophyseal lamina and ventrally by the paradiapophyseal lamina, and is placed ventrally to both infradiapophyseal and infraprezygapophyseal fossae. This fossa is absent in the first two dorsal vertebrae of *Shri devi* (Turner et al., 2021) and in the cervicodorsal vertebra of *Luanchanraptor henanensis* (Lü et al., 2007), and is considered an autapomorphy of *Shri rapax*. This fossa is topographically equivalent to the 'prezygapophyseal-paradiapophyseal fossa' *sensu* Gianechini and Zurriaguz (2021) reported in more caudally placed dorsal vertebrae of *Buitreraptor gonzalezorum* and *Unenlagia comahuensis*. The rest of the dorsal centra is still embedded in the sediments. Almost all dorsal ribs are in articulation with the vertebrae. In the dorsal ribs, the capitulum is rectangular in cross-section and its dorsal margin is slightly concave, leading to the articular facet for the tuberculum, which is also slightly concave. The shaft of the tuberculum does not extend more dorsally than the shaft of the capitulum, unlike in

Deinonychus antirrhopus (Ostrom, 1969). The ribs are slightly bowed caudally. A large sulcus is present cranioventrally. Approximately in the middle of their shaft, ossified uncinate processes are preserved on dorsals 3 to 8 and oriented caudolaterally. This feature is common among oviraptorids and dromaeosaurids (Codd et al., 2008). In dromaeosaurids, ossified uncinate processes or scars from their insertion have been observed in several taxa, e.g. *Microraptor zhaoianus*, *Deinonychus antirrhopus*, *Velociraptor mongoliensis* and *Saurornitholestes langstoni* (Codd et al., 2008; Norell & Makovicky, 1999; Ostrom, 1969; Xu et al., 2000, 2003). In MPC-D 102/117, most of them are broken, but the best-preserved ones are quite long, overlapping the following rib and being ventrolaterally flattened, recalling the condition in some flying birds (Tickle et al., 2007), except that they are not fused to the ribs. The uncinate processes are proportionally shorter than in *Velociraptor mongoliensis* (Norell & Makovicky, 2004).

Sacral vertebrae

The precise number (5 or 6) of sacral vertebrae is uncertain, because the sacrum is still partly embedded in the sediments and articulated with the pelvic girdle (Figure 5). The vertebrae seem to be co-ossified to form a synsacrum like in *Velociraptor mongoliensis* (Norell & Makovicky, 2004). The sacral spines are fused and form a continuous lamina dorsally. The contact of the sacral vertebrae with the iliac blades is only visible on the last two vertebrae.

Caudal vertebrae

The caudal series includes 23 articulated vertebrae (Figure 6): in eudromaeosaurs, the tail usually includes about 30–40 caudals, as in *Deinonychus antirrhopus* and *Velociraptor mongoliensis* (Norell & Makovicky, 1997; Ostrom, 1969). Although we cannot determine how many additional vertebrae were originally present distal to the 23rd caudal vertebra, the latter is assumed to be close to the end of the tail since its length is subequal to the average length of the first six caudal centra (as in dromaeosaurid posteriormost caudal vertebrae, Senter et al., 2012), the dorsoventral diameter of its cranial facet is half the average diameter of the preceding five vertebrae (marking an abrupt reduction in tail diameter), and it is not included in the bundle of elongate haemal processes which forms the caudotheca (Figure 6A,C; Senter et al., 2012, i.e. it is not ventrolaterally enclosed by elongate bony projections from subsequent vertebrae). Three rod-like extensions of the prezygapophyses are placed laterally to 21st and 22nd caudal centra (Figure 6B). In both cases, one rod is more robust than the others, and is interpreted as the proximal part of the right prezygapophysis of the subsequent vertebra. The two more slender rods are interpreted as the couple of bifurcating rods of the right prezygapophysis of a more-distally placed vertebra (see Ostrom, 1969). This implies that at least one missing vertebra was originally present distal to the 23rd position. Yet, we consider it unlikely that the caudotheca was originally extended further much distally, because only two rod-like haemal processes are visible adjacent to the 20th caudal centrum, and none is associated to the last two preserved vertebrae. The length of the vertebrae increases progressively along most of the caudal series, with the centra being increasingly flattened dorsoventrally. Yet, when compared to similarly-preserved caudal series of *Deinonychus* and *Velociraptor* (Norell & Makovicky, 1999; Ostrom, 1969), in *Shri rapax* the elongation of the caudal vertebrae distal to the transition point (i.e. positions 9th to 23rd) is less marked than in those eudromaeosaurs and intermediate between the latter taxa and some non-dromaeosaurid theropods such as ornithomimids and abelisaurids (see Discussion). The transition point occurs between caudals 6 and 8, a condition similar to some microraptorines and *Anchiornis huxleyi* (Pei et al., 2014, 2017). Proximal to the transition point, the caudal centra are proportionally shorter, with haemal arches inclined caudoventrally to the corresponding centrum (Figure 7A). The first caudal vertebra is overlapped laterally by the postacetabular blade of the ilium. The craniocaudal length to dorsoventral height ratio in the first eight caudal centra is between 1 and 2. The neural spines are well-developed and oriented caudodorsally, as in troodontids and other dromaeosaurids (Motta et al., 2018). The prezygapophyses are craniodorsally oriented, with their articular surface facing medially. Consequently, the articular facets of the postzygapophyses are oriented laterally as in *Velociraptor mongoliensis* (Norell & Makovicky, 1997). This condition differs from the horizontally oriented zygapophyses diagnostic for halszkaraptorines (Cau et al., 2017). The transverse processes are elongated and extended caudolaterally. Distal to the transition point, the centra become progressively more elongated (Figure 7B,C), with a ratio between 2 and 5.5 as in other dromaeosaurids (Motta et al., 2018). The neural spines are reduced to a scar on the middle dorsal surface on the vertebrae immediately distal to the transition point, as also observed in *Buitreraptor gonzalezorum*

and *Rahonavis ostromi* (Forster et al., 1998; Novas et al., 2018), then completely absent, as in other dromaeosaurids and basal avialans (Motta et al., 2018). The transverse processes progressively reduce in size and become a simple ridge at the level of the caudal 10, as in *Buitreraptor gonzalezorum*, beyond which they are absent, as in most paravians (Motta et al., 2018). The prezygapophyses are hyperelongated (Figure 7A,C) and form the caudotheca (Senter et al., 2012). The caudotheca is similar to most eudromaeosaurs and differs from the Jehol Biota dromaeosaurids in not extending cranial to the 6th tail vertebra (Senter et al., 2012; Wang et al., 2022). The postzygapophyses are directed dorsally and their articular surfaces face laterally. The first haemal arch is located just caudal to the first caudal centrum. It is elongated, tapered ventrally and narrow craniocaudally. As in most paravians, the centrum of caudal 1 is smaller than the dorsoventral length of the haemal arch (Motta et al., 2018). The inclination of the proximodistal axis of the first five haemal arches relative to the long axis of the tail changes progressively from strongly caudoventral to more or less perpendicular, similar to crocodilians and other theropods (e.g. Brochu, 2003; Turner et al., 2021). The second haemal arch is similar in shape to the first one. From the third onwards, the ventral end widens craniocaudally to form a platform, the ventral edge of which becomes concave distally as in the velociraptorine MPC-D 100/985 (Norell & Makovicky, 1997). This differs from both type specimens of *Luanchanraptor henanensis* and *Shri devi*, which have at least three haemal arches bearing the elongate ventrally-tapered morphology (Lü et al., 2007; Turner et al., 2021). There is also a trend for the height of these arches to decrease in dorso-ventral length and to increase in craniocaudal length as in troodontids, basal avialans and other dromaeosaurids (Motta et al., 2018). The subsequent haemal arches are bifurcated cranially and caudally (Figure 7A, B), with very elongated cranial processes that form the ventral part of the caudotheca. *Shri rapax* differs from *Deinonychus antirrhopus* and *Luanchuanraptor henanensis* in lacking an accessory median spur in the haemal arches (see fig. 41B in Lü et al., 2007; Ostrom, 1969).

Sternal plates

The sternal plates are often reported yet variably preserved in dromaeosaurids (e.g. Burnham, 2004; Cau et al., 2021; Norell & Makovicky, 1997; Wang et al., 2022). In this specimen, the paired sternal plates are nicely preserved in articulation, except for the right coracoidal facet, which is partly damaged (Figure 8A). The two plates are exposed ventrally and contact each other all along their medial margin. In *Bambiraptor feinbergi*, the plates are in contact only caudally (Burnham, 2004) but are not fused. The sternal plates look like those in *Velociraptor mongoliensis* and *Linheraptor exquisitus* (Norell & Makovicky, 1997; Xu et al., 2010) and are not as craniocaudally elongated as in *Halszkaraptor escuilliei* and *Bambiraptor feinbergi*, or the early saurischian *Tawa hallae* (Bradley et al., 2019; Burnham, 2004; Cau et al., 2021). Each plate is twice as long as wide (at maximum width proximally). Their distal edge is also convex, and the two plates meet slightly more cranially than their distal point. They are flat to slightly curved ventrally and just a little bit concave proximally. Two pairs of foramina open in the cranial half of their ventral surface. The two coracoidal facets are convex and oriented mediolaterally. Their lateral edge is wave-shaped: the plate is wider proximally, then the edge is concave, becoming convex distally at about half the craniocaudal length. Four pairs of sternal ribs are preserved and attached to the sternal plates through four costal processes on the lateral sides on the plates like in other dinosaurs (e.g. *Tawa hallae*, Bradley et al., 2019: *Daurlong wangi*; Wang et al., 2022). The lateral trabecula is not marked, and the caudal margins are not straight as an isolated sternal plate described by Godfrey and Currie (2004), but more convex.

Gastralia

The specimen preserves the articulated gastral basket, directly distal to the two sternal plates (Figure 8B). It includes 15 pairs of gastral segments. The nine first pairs are aligned with the sternal plates and the other ones are disarticulated laterally. Each segment is composed of a medial part imbricated to the lateral part, except for the first pair which is thicker and bears only the medial part. The first two pairs overlap the caudal margin of the sternal plates. The proximal ends of the medial parts are bifurcated and overlap the preceding, similar to other theropods (e.g. *Velociraptor mongoliensis* MPC-D 100/985). This configuration forms a zigzag pattern, aligned with the midline of the sternal plates. The distal ends of the lateral parts are tapered. The medial part of the segments is shorter than the lateral ones, which is also the condition in *Velociraptor mongoliensis* (Norell & Makovicky, 1997).

Furcula

The furcula is well preserved except for the omal end of the right ramus, and it is only visible in cranial view

(Figure 9A,C). The furcula shows a flared 'U'-shape as in *Sinornithosaurus millenii*, *Bambiraptor feinbergi* and *Buitreraptor gonzalezorum* (Burnham, 2004; Gianechini et al., 2018; Xu, 2002). It is compressed craniocaudally as in the former two taxa (Burnham et al., 2000; Xu et al., 1999). The two rami of the furcula are oriented latero-dorsally and form an angle of approximately 75°, similar to *Sinornithosaurus millenii*, *Bambiraptor feinbergi* and *Buitreraptor gonzalezorum* (Burnham, 2004; Gianechini et al., 2018; Xu et al., 1999). Each ramus tapers omally (distally) as in *Velociraptor mongoliensis* and *Microraptor zhaoianus* (Nesbitt et al., 2009). The epicleideal processes seem continuous with the rami like in *Sinornithosaurus millenii*, *Bambiraptor feinbergi* and *Archaeopteryx lithographica* (Burnham et al., 2000; Mayr et al., 2007; Xu et al., 1999). The furcula does not appear to bear a distinct hypocleidium, as in *Bambiraptor feinbergi* and unlike the distinct process in *Buitreraptor gonzalezorum* and *Halszkaraptor escuilliei* (Cau et al., 2021; Makovicky et al., 2005).

Scapula

Only the left scapula is preserved (Figure 9). It is very similar to that of *Sinornithosaurus millenii* (Xu et al., 1999). The angle between the scapula and the coracoid is less than 90°. The length of the scapula is approximately 98% of the humeral length, greater than in *Deinonychus antirrhopus* (about 84%; Ostrom, 1969), *Buitreraptor gonzalezorum* (70%; Gianechini et al., 2018), *Microraptor zaoianus* (68%; Hwang et al., 2002), and approaching *Linheraptor exquisitus* (about 103%, Xu et al., 2010). The scapular blade is elongated, strap-like, and medio-laterally compressed, comparable to most dromaeosaurids (e.g. *Bambiraptor feinbergi*, *Sinornithosaurus millenii*; Burnham, 2004; Xu et al., 1999) (Figure 9A). Its dorsal and ventral margins are parallel and the blade mediolaterally tapers distally like in *Unenlagia comahuensis* (Novas et al., 2021). The blade is bowed proximally, more ventrally than dorsally and becomes straight distally, like in *Velociraptor mongoliensis* (Norell & Makovicky, 1999). The distal end is square with rounded corners, similar to *Deinonychus antirrhopus* (Ostrom, 1969). The scapula is not fused to the coracoid, but the coracoid facet occupies the whole height of the cranial border of the scapula. The proximal plate of the scapula is mediolaterally wider than the blade, as in *Buitreraptor gonzalezorum* (Gianechini et al., 2018). The glenoid fossa of the scapula is bordered ventrally and caudally by a rim, as in *Buitreraptor gonzalezorum* and *Unenlagia comahuensis* (Gianechini et al., 2018; Novas et al., 2021); it is latero-ventrally oriented as in *Sinornitholestes millenii*, *Buitreraptor gonzalezorum*, *Bambiraptor feinbergi* and *Velociraptor mongoliensis* (Burnham, 2004; Gianechini et al., 2018; Norell & Makovicky, 1999; Xu et al., 1999) (Figure 9B). The contribution of the scapula to the glenoid fossa is approximately 1.5 times larger than the coracoid contribution. The craniodorsal border of the glenoid fossa of the scapula bears a deep concavity, tentatively identified by Gianechini et al. (2018) as the insertion area for the glenohumeral ligament. As in *Buitreraptor gonzalezorum* and *Bambiraptor feinbergi* (Burnham, 2004; Gianechini et al., 2018), the lateral side of the scapula between the glenoid fossa and the acromion process is concave. The latter process is triangular in lateral view and its proximal end is continuous with the scapula distally, and projects into the coracoid at the level of the scapula-coracoid suture proximally. This projection of the scapula into the coracoid is typical of many paravians, including *Unenlagia comahuensis*, *Sinornithosaurus millenii* or *Bambiraptor feinbergi* (Gianechini et al., 2018).

Coracoid

Both coracoids are present, with the left one still articulated with the scapula (Figure 9). The coracoid is subquadrangular with a large articular surface for the scapula and a large articular surface for the sternal plate, similar to *Deinonychus antirrhopus, Sinornithosaurus millenii* and *Saurornitholestes langstoni* (Jasinoski et al., 2006; Ostrom, 1974; Xu et al., 1999). In lateral view, it is 'L'-shaped, because the proximal part bearing the articular surface for the scapula is perpendicular to the distal surface housing the articulation for the sternal plate. The bone is concave laterally and convex cranially. The coracoid bears a strong cranioventral projection at the level of the supraglenoid fossa, like in *Deinonychus antirrhopus* (Ostrom, 1974). The glenoid facet is oriented proximolaterally. The subglenoid fossa is hook-shaped and tapers distally. The ventral part of the latter is marked by a ridge joining the posterior coracoid process distally. The posterior coracoid process differs from the hook-shaped morphology of *Saurornitholestes langstoni* and *Deinonychus antirrhopus* (Jasinoski et al., 2006; Ostrom, 1974), being more rounded like in *Sinornithosaurus millenii* (Xu et al., 1999). This process is connected to the coracoid ('bicipital') tubercle through a straight ridge. This large and rounded tubercle is placed proximomedially to the subglenoid fossa, like in *Saurornitholestes langstoni* (Jasinoski et al., 2006). Distally, a large supracoracoid fenestra is present, as in microraptorines and *Luanchuanraptor henanensis* (Lü et al., 2007; Xu et al., 1999). The supracoracoid fenestra is oriented latero-medially, and is proportionally much larger than that

in *Sinornithosaurus millenii* (Xu et al., 1999). It is teardrop-shaped and occupies a large part of the distal surface of the coracoid (Figure 9A,B). The supracoracoid foramen is present in the proximal part of the coracoid (Figure 9B). The facet for the sternum is convex and curves medially, with the ventral surface of the cranial part being strongly concave, both features like in *Sinornithosaurus millenii* (Xu et al., 1999).

Humerus

The entire right forelimb is preserved and exposes its lateral side (Figure 10). The humerus is in articulation with the scapulocoracoid proximally and with ulna and radius distally. The proximal end of humerus is large and slightly concave laterally, less than in *Unenlagia* (Novas et al., 2021) but similar to *Bambiraptor feinbergi* and *Deinonychus antirrhopus* (Burnham et al., 2000; Ostrom, 1969). Its proximal end is compressed craniocaudally. The humeral head is not projected laterocaudally, unlike in *Unenlagia comahuensis* (Novas et al., 2021), more closely resembling the condition in *Bambiraptor feinbergi* (Burnham et al., 2000). The shape of the proximal edge along the head to the deltopectoral crest is very similar to the condition in *Bambiraptor feinbergi* (Burnham et al., 2000). The humerus has a low yet well-developed deltopectoral crest, projected cranially as in *Austroraptor cabazai* (Novas et al., 2009) and *Deinonychus antirrhopus* (Ostrom, 1969). This crest has a trapezoidal shape, very similar although more developed than in *Bambiraptor feinbergi* (Burnham et al., 2000) (Figure 9B), and is located in the proximal quarter of the humerus. The ventral edge forms an angle of approximately 140° with the shaft, similar to the condition in *Buitreraptor gonzalezorum* and *Austroraptor cabazai* (Gianechini et al., 2018) but more cranially oriented in relation to the shaft than in *Bambiraptor feinbergi* (Burnham et al., 2000). The caudal part of the proximal end, behind the humeral head, is not visible. The humeral shaft is straighter than in *Buitreraptor gonzalezorum* (Gianechini et al., 2018) in lateral view, while its proximal part is slightly curved caudolaterally, more than in *Unenlagia comahuensis*. The distal part of the shaft is gently curved cranially like in *Bambiraptor feinbergi* (Burnham et al., 2000). As in *Unenlagia comahuensis* (Novas et al., 2021), the proximal and the distal ends do not extend in the same plane, differing from crown-ward avialans in which the proximal and the distal ends of the shaft are aligned in the same plane. Laterally, a large flange is present, extending from the apex of the deltopectoral crest, running parallel to the caudal edge of the bone before shifting more laterally in its distal end. This flange is better marked than in other eudromaeosaurs but is similar to the one of *Unenlagia comahuensis*, suggesting a prominent insertion for *M. deltoideus scapularis* (Jasinoski et al., 2006). The distal end is craniolaterally to caudomedially oriented, as also preserved in other dromaeosaurids like *Austroraptor cabazai* or *Deinonychus antirrhopus* (Novas et al., 2009; Ostrom, 1969). The ulnar and the radial condyles seem paralleling each other (the ulnar condyle is partially hidden behind the proximal end of the ulna). The condyles are separated by a shallow cranial groove (Figure 10C) as in *Buitreraptor gonzalezorum* and *Bambiraptor feinbergi* (Burnham et al., 2000; Gianechini et al., 2018).

Ulna

The right ulna is complete but, like the humerus, only its lateral side and part of its medial shaft are visible (Figure 10A). It is in articulation with the humerus and the radius as well as with carpal bones. Its length is about 88% of the humerus length. The shaft is distinctly bowed caudolaterally, more than in *Deinonychus antirrhopus* (Ostrom, 1969). The distinct curvature of the ulna is diagnostic for pennaraptorans (Gianechini et al., 2018). The ulnar shaft is compressed mediolaterally proximally and becomes rounder distally. It is more robust than in *Bambiraptor feinbergi* (Burnham, 2004). Like in *Mahakala omnogovae*, *Velociraptor mongoliensis*, *Bambiraptor feinbergi* and *Buitreraptor gonzalezorum*, a longitudinal ridge extends along its caudal surface (Burnham, 2004; Gianechini et al., 2018; Norell & Makovicky, 1999; Turner et al., 2011). In lateral view, its proximal end is partly hidden by the articulation with the radius and the sedimentary matrix. The lateral articular surface is convex. The olecranon extends more proximally than the articular facets (Figure 10B), which is comparable to *Buitreraptor gonzalezorum* and *Bambiraptor feinbergi* (Burnham, 2004; Gianechini et al., 2018). A bicipital scar is present along the cranial part of the shaft in lateral view, also found in *Buitreraptor gonzalezorum* and *Mahakala omnogovae* (Gianechini et al., 2018; Turner et al., 2011). Distally, the craniolateral part of the shaft becomes flat at the radius insertion and a distal flange separates this surface from the rest of the shaft. This flat surface forms a triangle opened distally and which begins at approximately halfway along the shaft, similar to *Buitreraptor gonzalezorum*, *Bambiraptor feinbergi* and *Mahakala omnogovae* (Burnham, 2004; Gianechini et al., 2018; Turner et al., 2011). The distal articular surface is rounded laterally. Unlike in *Deinonychus antirrhopus*,

in which the distal end is compressed lateromedially (Ostrom, 1969), it is compressed craniocaudally.

Radius

The right radius is exposed in lateral view (Figure 10A). It is in articulation with the ulna, humerus and the proximal carpal bone (scapholunare). The shaft is straight, although its distal part is slightly curved cranially. The same orientation is also reported in one specimen of *Buitreraptor gonzalezorum* and considered by Gianechini et al. (2018) as a taphonomic artefact. Yet, the cranial curvature of the distal part of the shaft in *Shri rapax* can nevertheless be observed also in *Deinonychus antirrhopus* (Ostrom, 1969). The shaft of the radius is about as wide as the distal half of the ulnar shaft, similar to the condition in *Deinonychus antirrhopus* (Ostrom, 1969), and differing from most paravians, including several non-eudromaeosaurian dromaeosaurids (e.g. *Austroraptor cabazai*, *Bambiraptor feinbergi*, *Halszkaraptor escuilliei*, *Mahakala omnogovae*, *Microraptor zahoianus*), in which the shaft of the ulna is significantly wider than the radius (Burnham, 2004; Cau et al., 2017; Gianechini et al., 2018). Both its proximal and distal ends are widened craniocaudally relative to the shaft. The proximal end is poorly observable but seems rounded. A small process is present on the lateral shaft and directed laterally below the articulation and superimposed on the lateral surface of the ulna, a feature also present in *Buitreraptor gonzalezorum* and *Rahonavis ostromi* (Forster et al., 2020; Gianechini et al., 2018). The distal end is flattened medio-laterally. It seems to be divided in two parts like in *Bambiraptor feinbergi* (Burnham, 2004). The caudal part of the distal end is better developed distally than the cranial one and is hook-shaped. The cranial part is rounder. Between these two parts, there is a shallow concavity.

Carpals

Only two carpals are present (Figure 10A). They are stacked one on top of the other. The proximal one (scapholunare; Botelho et al., 2014) articulates with the ulna and the radius while the distal one (semilunate; Botelho et al., 2014) articulates with the metacarpals. The scapholunare is oval and smaller than the semilunate. It articulates with the ulna caudally and with the radius in the caudal part of the proximal end. It was probably articulated with the radius over most of its proximal part, and somewhat disarticulated during fossilisation. The distal end is in contact with the semilunate. The latter is around 1.3 times wider craniocaudally than the scapholunare. It is 'D'-shaped, with the rounded part pointing proximally at the level of the articulation with the scapholunare. This articulation is made only on the centre of the latter. Distally, it is articulated with both metacarpals I and II (a possible articulation with metacarpal III cannot be determined). Metacarpal II articulates on the caudal distal facet, while metacarpal I articulates on the distal cranial facet.

Manus

The right manus is complete, articulated and bears three fingers (Figures 10A, 11). It is mainly exposed in ventral view. The first metacarpal is the shortest but also the most robust metacarpal, being about half the length of metacarpal II but almost twice as wide, a condition unique to *Shri rapax* among paravians, which usually bear a relatively slenderer element (e.g. Norell & Makovicky, 1999; Ostrom, 1969). In ventral view, the shaft is slightly concave transversely, wider proximally than distally. The distal medial part of the shaft is concave. The exposed margin of the proximal surface is flat to moderately concave for the articulation with the semilunate carpal. Its distal end is concave with two ventrally developed and rounded condyles for the articulation with the first phalanx. This ginglymoid shape is asymmetric because the lateral condyle is more developed than the medial one, unlike in *Bambiraptor feinbergi* (Burnham, 2004), in which the medial one is better developed. The distal articular facet is similar to that of *Deinonychus antirrhopus* (Ostrom, 1969), differing in the more parallel orientation of the condyles. The shaft of metacarpal II is more symmetrical than that of the first metacarpal and very slightly bowed dorsally. In ventral view, its proximal part is overlapped by metacarpal I medially and by metacarpal III laterally. The proximal articular facet is convex for the contact with the semilunate carpal. The distal end is ginglymoid like in *Deinonychus antirrhopus* and *Velociraptor mongoliensis* (Norell & Makovicky, 1999; Ostrom, 1969), and asymmetrical, with the lateral condyle larger than the medial one, like in *Bambiraptor feinbergi* (Burnham, 2004) but unlike *Deinonychus antirrhopus* and *Velociraptor mongoliensis* in which the medial condyle is larger. Metacarpal III is the thinnest (less than half the width of metacarpal II) and is slightly shorter than metacarpal II. It is more curved dorsally than the other two. The proximal articular facet is not visible. The distal end is similar to that of metacarpal II in bearing an asymmetrical ginglymoid articular facet. On these three metacarpals, the ligament pits are either not visible or only slightly developed.

Phalanges

The phalangeal formula is 2–3–4-x-x (Figure 11), the usual tetanuran and dromaoesaurid pattern (Norell & Makovicky, 1999; Ostrom, 1969). Manual ungual 2 was

missing and has been reconstructed (compare Figures 1 and 11). The preserved manual unguals are falciform, proportionally large, pointed and ventrally curved, as in other dromaeosaurids (Norell & Makovicky, 2004). The first finger is markedly more robust than the other two fingers, unlike *Bambiraptor feinbergi*, *Deinonychus antirrhopus* and *Velociraptor mongoliensis* (Burnham, 2004; Norell & Makovicky, 1999; Ostrom, 1969) in which the first two fingers are more similar in robustness. The penultimate phalanx is the longest on each digit, as usual in most theropods, incuding the other eudromaeosaurs (e.g. Ostrom, 1969). Like in *Deinonychus antirrhopus*, all phalanges have well developed ginglymoid articular facets and in most cases distinct ligaments pits distally (Ostrom, 1969). Phalanx I-1 is unique among paravians in being very robust and markedly stockier than the first phalanx in the other fingers (e.g. compare it with the more gracile condition in *Velociraptor mongoliensis*, Norell & Makovicky, 1999). This condition more closely resembles the basal alvarezsauroids (Choiniere et al., 2010) and other non-paravian tetanurans (e.g. *Megaraptor namunhuaiquii*; Calvo et al., 2004) than the other dromaeosaurids. The distal width of the phalanx is 26% of bone length, more robust than in other dromaeosaurids (17% in *Velociraptor mongoliensis*, 21% in *Deinonychus antirrhopus*; Norell & Makovicky, 1999; Ostrom, 1969). Its proximal part is slightly curved dorsally. The lateral part of its ventral side is irregular, which might be pathological. Its lateral edge is proximally concave, then convex, becoming straight distally. The proximal articulation is convex. Ventrally, a deep groove marks the distal end, as in *Deinonychus antirrhopus* (Ostrom, 1969). In the distal end, the lateral condyle is larger than the medial one, and both condyles are bound by distinct collateral pits. The first ungual is extremely enlarged and falciform, measuring along the outer margin more than 162% the length of the preceding phalanx, and more than 730% of the dorsoventral diameter of the ungual proximal facet. Both ratios are significantly larger than in *Velociraptor mongoliensis* (respectively, 100% and 211%, Norell & Makovicky, 1999) and *Deinonychus antirrhopus* (respectively, 126% and 395%; Ostrom, 1969). The first ungual bears a large and rugose flexor tubercle projected ventrally, similar to but proportionally larger than in *Velociraptor mongoliensis* (Norell & Makovicky, 1999), and a deep collateral groove. In overall proportions, phalanx II-1 is quite similar yet more robust than those of *Deinonychus antirrhopus* and *Velociraptor mongoliensis* (Norell & Makovicky, 1999; Ostrom, 1969). It is quite symmetric with both ends allowing a ginglymoid articulation. Distally, the lateral condyle is slightly larger than the medial one, as in *Velociraptor mongoliensis* (Norell & Makovicky, 1999). Phalanx II-2 is similar to II-1, being slightly longer, and bearing deep collateral ligament pits distally. The phalanges of digit III are proportionally more robust than those in *Velociraptor mongoliensis* (Norell & Makovicky, 1999). Phalanx III-2 is stout and the shortest phalanx of the manus, as is usual in dromaeosaurids (e.g. Norell & Makovicky, 1999; Wang et al., 2022). Articulations are ginglymoid but asymmetric for phalanges 1 and 2. Phalanx III-3 is proportionally the most gracile phalanx of the digit, very similar to the penultimate phalanx of digit II although slightly shorter. Compared to the first ungual, the third manual ungual is proportionally shallower than in *Velociraptor mongoliensis* and more similar to *Deinonychus antirrhopus* (i.e. the height of the proximal facet is 70% that of the first ungual, compared to 88% in *Velociraptor mongoliensis*, and 72% in *Deinonychus antirrhopus*; Norell & Makovicky, 1999; Ostrom, 1969).,

Pelvic girdle

The pelvis is completely articulated (Figures 5, 12A, B). It is particularly well preserved, even if both ilia are partially damaged especially on their craniodorsal part and at the junction with the pubis for the right one. The latter is also partially damaged at the level of the pubic peduncle. The proximal and distal parts of pubes are slightly eroded. Both ischia are essentially complete. The pubis is distinctly retroverted, as in other dromaeosaurids (Norell & Makovicky, 1997): the angle between the long axis of the ilium and the midline of the pubis is about 135° in lateral view. *Shri rapax* differs from the more extreme opisthopubic condition present in the holotype of *Shri devi* and in the articulated specimens of *Velociraptor mongoliensis* (155–160°; Norell & Makovicky, 1997; Turner et al., 2012). We consider the difference in the inclination of the pelvic bones between MPC-D 102/117 (*Shri rapax*) and MPC-D 100/980 (*Shri devi*, Turner et al., 2021) not significantly altered by taphonomic processes because in both specimens: (1) the long axis of the first haemal arch is not inclined as the other haemal arches but is aligned with the long axis of the ilium, as expected in articulated and undeformed theropod skeletons (see Brochu, 2003); (2) the cloacal angle described by the first haemal arch with the long axis of the ischium is about twice the angle formed by the latter with the long axis of pubis, as in other articulated dromaeosaurid skeletons (e.g. MPC-D 100/985, Norell & Makovicky, 1997; *Microraptor*; Xu et al., 2003); (3) the elliptical outline of the acetabulum is poorly depressed and is completely encircled by the articulated pelvic bones; (4) the distal tip of the ischium is placed slightly cranial to the line linking the tip of the

first haemal arch and the ventrodistal corner of the pubic foot, a configuration in agreement with other articulated skeletons and with the expected extent in life of the *M. caudotruncus* in dromaeosaurids (Carrier & Farmer, 2000; Norell & Makovicky, 1997; Xu et al., 2003).

Ilium

The ilium is dolichoiliac as in all neotheropods (Figure 12). The extremities of the blades are slightly bent ventrally, as in *Shri devi* and *Bambiraptor feinbergi* (Burnham, 2004; Turner et al., 2021). The margin of the cranial end is partially damaged, yet, the photographs of the specimen prior to 2016 show that originally the cranial margin was convex, much like in *Velociraptor mongoliensis* and more angular than in *Shri devi* (Norell & Makovicky, 1997; Turner et al., 2021) due to the presence of an acute craniodorsal corner (see Figure 1). The medial antiliac shelf is absent, a condition approached by *Shri devi* among dromaeosaurids (Novas, 2004, *contra* Norell & Makovicky, 1997; Turner et al., 2021). As in other dromaeosaurids, the cranial portion of the ilium is slightly longer than the caudal one at the midpoint of the acetabulum probably due to the broad pubic peduncle. The pubic peduncle is concave, more 'C'-shaped than in *Velociraptor mongoliensis* (MPC-D 100/985) and its lateral surface is directed craniolaterally. The caudal margin of the pubic peduncle is bent caudoventrally and forms the cranial part of the acetabulum. The contact facet for the pubis is oriented ventrally as in *Shri devi* (Turner et al., 2021). The right ischiadic peduncle is totally damaged, yet the better preserved left ilium shows a reduced supracetabular ridge as in other dromaeosaurids (e.g. Norell & Makovicky, 1999).

Pubis

The pubes (Figure 12) are proportionally shorter than those reconstructed for the holotype of *Shri devi* (Turner et al., 2021) and differ in the more moderate degree of the opisthopubic condition. The extreme condition of *Shri devi* is reported in well-preserved specimens of *Velociraptor mongoliensis* (Norell & Makovicky, 1997), and has been considered a derived feature shared by the two taxa (Turner et al., 2021). The pubes of the two *Shri* species also differ each other in the inclination of the cranial margin of the iliac peduncle, which in *Shri rapax* is less inclined caudoventrally relative to the long axis of the ilium (about 30° *vs* 45° in *Shri devi*). The proximal half of each pubis is compressed laterally, then it widens before contacting the other one to form the fused pubic apron (Figure 12B). The cranial part of the proximal end is eroded so the *M. ambiens* attachment site cannot be observed. The apron extends from the cranial edge of the shaft for about half of the pubis (minimum value, not including the pubic foot). The cranial surface of the pubic apron is concave in proximal view. The margin of the pelvic canal described by the apron is flexed caudodorsally, approaching the corresponding margin described by the obturator process of the ischium. Although the midline of the cranial surface of the pubic apron houses a proximodistally-oriented sulcus, there is no evidence of an interpubic fenestra. Only the proximal part of the pubic feet is sufficiently preserved, showing a caudal projection similar to other dromaeosaurids (e.g. Norell & Makovicky, 1999).

Ischium

Both ischia are well preserved (Figure 12), and resemble the condition in *Velociraptor mongoliensis* and *Deinonychus antirrhopus* (Norell & Makovicky, 1997; Ostrom, 1969). The ischia are quite elongated being 67% of pubic length versus 54–59% in *Velociraptor mongoliensis* and about 50% in *Shri devi* (Norell & Makovicky, 1997; Turner et al., 2021). The iliac peduncle is more convex than in *Deinonychus antirrhopus* (Ostrom, 1969). The pubic peduncle is straight and directed cranioventrally as in *Deinonychus antirrhopus* (Ostrom, 1969). The small cranial tubercle reported in *Velociraptor mongoliensis* and *Shri devi* is absent (Norell & Makovicky, 1997; Turner et al., 2021). The lateral surface of the ischium bears a sharp shelf extending along its proximal half, topographically equivalent to the lateral ridge in *Velociraptor mongoliensis* and *Shri devi* (e.g. Norell & Makovicky, 1999; Turner et al., 2021). This process in *Shri devi* is described as a rounded ridge (Turner et al., 2021), whereas the sharp shelf of *Shri rapax* is more similar to the condition in *Velociraptor mongoliensis* MPC-D 100/985 (see Figure 12 in Norell & Makovicky, 1997). The lateral margin of the shelf is gently convex in dorsal view. The dorsal surface of the shelf describes an elongate and dorsolaterally-facing depression with the lateral surface of the bone. The obturator process is broad and starts approximately at the middle of the ischium, differing from the more elongate process in *Shri devi* which occupies two thirds of the ischium (Turner et al., 2021). The cranial edge is blade-shaped and the obturator process forms a distinct tip, more pronounced than in *Velociraptor mongoliensis* (Norell & Makovicky, 1997). The caudal edge is gently sigmoid in lateral view, more convex proximally in the area topographically equivalent to the proximodorsal process of other paravians (e.g. *Rahonavis ostromi*;

Forster et al., 2020), and bent backwards distally, differing from the straight edge in *Shri devi* (Turner et al., 2021; Figure 12A). As in *Velociraptor mongoliensis* (Norell & Makovicky, 1997), the distal part of the ischium of *Shri rapax* caudal to the obturator notch diverges distally from the distal half of the pubis when seen in lateral view, differing from *Shri devi* where the distal ends of pubis and ischium are subparallel in lateral view (Turner et al., 2021). The paired ischia are not fused even though they contact distally (Figure 12B).

Femur

Only the proximal part of the right femur (Figure 13) and the distal part of the left femur (Figure 14) are preserved. Like other dromaeosaurids, the femoral shaft is bowed cranially, although far less than in *Velociraptor mongoliensis* (Norell & Makovicky, 1999) and *Shri devi* (Turner et al., 2021), more closely resembling the condition in *Deinonychus antirrhopus* (Ostrom, 1976) and *Neuquenraptor argentinus* (Novas & Pol, 2005). The proximal end of the right femur is similar to other dromaeosaurids, even if the part leading to the femoral head tapers medially and is less robust than *Velociraptor mongoliensis* (Norell & Makovicky, 1999). The femoral head is perpendicular to the craniocaudal axis of the femur, like in *Velociraptor mongoliensis* (Norell & Makovicky, 1999). There is no distinct neck that separates the head and the shaft, similar to the condition of *Buitreraptor gonzalezorum* (Gianechini et al., 2018) and *Rahonavis ostromi* (Forster et al., 2020). The head is compressed craniocaudally and is slightly convex ventrally. In proximal view, the femoral head is placed in the caudalmost portion like in *Velociraptor mongoliensis*, *Unenlagia comahuensis* and *Buitreraptor gonzalezorum* but unlike *Rahonavis ostromi* (Novas et al., 2021). Laterally, the shaft is expanded to form the greater trochanter. It is the proximalmost point of the bone, like in *Buitreraptor gonzalezorum* (Gianechini et al., 2018). Parallel to the greater trochanter, the lesser trochanter forms a well-developed ridge compressed medio-laterally, similar to the condition in *Unenlagia comahuensis* (Novas et al., 2021). The surface between the two trochanters is not depressed. The lesser trochanter is fused to the greater trochanter to form a trochanteric crest, much better developed than in *Rahonavis ostromi* (Forster et al., 2020). In lateral view, the proximocaudal portion is more rounded than in *Unenlagia comahuensis* (Novas et al., 2021), resembling the condition in *Rahonavis ostromi* (Forster et al., 2020). On the caudal surface of the shaft, just below the insertion of the femoral head, two small 'V'-shaped ridges can be seen, with their tips pointing proximally. They might correspond to a vestige of the fourth trochanter as it has been suggested for *Buitreraptor gonzalezorum* (Gianechini et al., 2018). The right femoral shaft is slightly compressed medio-laterally. The distal end of the left femur is well preserved. On its caudal surface, the medial condyle is separated from the lateral one by a deep longitudinal groove, forming the popliteal fossa, delimited by the medial condyle and the ectocondylar tuberosity. The lateral condyle is larger than the medial one, with the latter oriented craniocaudally and compressed medio-laterally. In medial view, the medial condyle is rounded. The lateral condyle is rounded and extended ventrolaterally, more ball-shaped and pronounced than in other dromaeosaurids (e.g. *Velociraptor mongoliensis*, *Unenlagia comahuensis*, *Buitreraptor gonzalezorum*, *Rahonavis ostromi*; Novas et al., 2021). The ectocondylar tuberosity (tibiofibular condyle) is extended caudally and compressed mediolaterally. In distal view, it is parallel to the lateral condyle and perpendicular to the medio-lateral plane of the femur. In lateral view, the ectocondylar tuberosity is rectangular and its distal margin is slightly concave at the junction with the lateral condyle. It is placed more medially than in *Bambiraptor feinbergi* (Burnham et al., 2000) and *Buitreraptor gonzalezorum* (Gianechini et al., 2018), better developed caudally than in *Deinonychus antirrhopus* (Ostrom, 1976) and more dorsoventrally elongated than in *Velociraptor mongoliensis* (Norell & Makovicky, 1999). It is similar to *Rahonavis ostromi* (Forster et al., 2020) but more extended caudally, and more flattened mediolaterally than in *Shri devi* (Turner et al., 2021). Like in *Buitreraptor gonzalezorum* and *Unenlagia comahuensis*, this tuberosity extends to the same level as the medial condyle. The cranial surface of the distal end of the femur is more concave than in *Unenlagia comahuensis* (Novas et al., 2021), bearing an extensor groove extending to the tip of its distal end.

Morphometric analysis

The result of the Principal Component Analysis of the caudal vertebrae measurements is shown in Figure 15. The Components 1, 2 and 3 describe, respectively, 66.67%, 17.4% and 6.03% of the variance. The analysis supports the hypothesis that in the dromaeosaurid caudal series, the elongation of caudal centra 9th to 20th relative to the proximal central is more marked than in other theropods (e.g. abelisaurids, ornithomimids). Yet, compared to the other dromaeosaurids sampled (i.e. *Deinonychus*, *Velociraptor*), the middle caudal vertebrae of *Shri rapax* are proportionally less elongate, providing a smaller contribution to tail elongation: as shown by Figure 15, the new taxon plots in a morphospace region

intermediate between those occupied by the non-dromaeosaurid and the dromaeosaurid samples.

Phylogenetic analysis

The analysis found 24 shortest trees of 1618 steps each (Consistency Index excluding uninformative characters = 0.4135; Retention Index = 0.4668). The strict consensus of all shortest trees is well-resolved and supports the monophyly of the five dromaeosaurid subfamilies (*sensu* Cau et al., 2017) (Figure 16). The topology resulted by the analysis differs from previous studies (Cau et al., 2017; Powers et al., 2021; Wang et al., 2022) in placing the '*Tianyuraptor*-like' taxa among the microraptorines, and the saurornitholestines among Dromaeosaurinae. Enforcing the '*Tianyuraptor*-like' taxa closer to eudromaeosaurs than microraptorines (as in Wang et al., 2022) is four steps less parsimonious than the shortest unenforced topologies. Enforcing the saurornitholestines outside the 'dromaeosaurine-velociraptorine' node (as in Powers et al., 2021) is six steps less parsimonious than the shortest unenforced topologies. In all shortest trees found, *Shri rapax* is reconstructed as sister taxon of *Shri devi* among Velociraptorinae. This node is well-supported and is diagnosed by seven unambiguous synapomorphies (jugal fitting into 'V'-shaped cleft of maxilla, postorbital bar more robust at mid-height than preorbital bar, distinct posterodorsal process of dentary, elongate external mandibular fenestra, reduced surangular-angular contact, medially confluent cervical postzygapophyses, accessory pleurocoel in cervicodorsal centra). The species *Velociraptor mongoliensis* is reconstructed as sister taxon of the genus *Shri* (as in Czepiński, 2023; Napoli et al., 2021; Turner et al., 2021). The other *Velociraptor* species, *Velociraptor osmolskae* (Godefroit et al., 2008), is reconstructed as closer to the node formed by *Tsaagan* and *Linheraptor*, a relationship also obtained by Powers et al. (2021).

Discussion

The exceptional completeness, uninterrupted articulation of the entire axial column, and exquisite three-dimensional preservation in a dinosaur skeleton the size of MPC-D 102/117 is a peculiar taphonomic pattern observed only in some specimens from the Djadokhta lithobiotope among the Nemegt Basin units (Jerzykiewicz et al., 2021). This taphonomic pattern is causally linked to the peculiar abundance of paedogenic calcite widespread in the structureless sandstone facies present in this unit, which plays a pivotal role in explaining the preservation of well-preserved, articulated, and unscavenged vertebrate skeletons (Dingus et al., 2008). As discussed by Jerzykiewicz et al. (2021), such mix of taphonomic and facies conditions is diagnostic of the Djadokhta lithobiotope and is not associated to any fossiliferous facies from the Baruungoyot or Nemegt formations. Examples of theropods from the Djadokhta Formation or from lithologically-analogous Chinese units (e.g. Wulanshuai Formation, Xu et al., 2010) found in a state of preservation comparable to the new dromaeosaurid include *Velociraptor mongoliensis* MPC-D 100/25 (see Carpenter, 2000), *Khaan mckennai* MPC-D 100/1127 and MPC-D 100/1002 (Balanoff & Norell, 2012), *Halszkaraptor escuilliei* MPC-D 102/109 (Cau et al., 2017), and *Linheraptor exquisitus* IVPP V16923 (Xu et al., 2010). It is noteworthy that all dromaeosaurids from the Baruungoyot Formation, including both specimens of *Shri devi*, are more disarticulated and less complete than the new specimen here described, and do not show such an exceptional level of preservation (e.g. Cau & Madzia, 2018; Czepiński, 2023; Lee et al., 2022; Napoli et al., 2021; Osmólska, 1982; Turner et al., 2021). We thus refer the new theropod to a fossiliferous facies from the Djadokhta Formation.

The specimen MPC-D 102/117 is unambiguously referred to Dromaeosauridae based on the presence of a posterodorsally extended subnarial ramus of the premaxilla (Barsbold & Osmólska, 1999), a splenial exposed in lateral view (Barsbold & Osmólska, 1999; Norell et al., 2006), dorsal ribs with uncinate processes (e.g. Norell & Makovicky, 1999), caudal vertebrae with extremely elongate prezygapophyses and haemal arches (Ostrom, 1969), paired and enlarged sternal plates (Norell & Makovicky, 1999); an abbreviated second phalanx of the third finger (Norell & Makovicky, 1999; Ostrom, 1969), high arching of the dorsal margin of the manual unguals (Senter et al., 2012), and a strongly caudoventrally oriented pubis (Norell & Makovicky, 1999; Turner et al., 2021). Several synapomorphies among the dromaeosaurids from the Nemegt units are shared by MPC-D 102/117 and the hypodigm of *Shri devi* (Czepiński, 2023; Turner et al., 2021), including the relatively shorter snout with the antorbital fenestra not longer than tall, the angular posterior margin of the maxillary fenestra, the 'Z'-shaped jugal-maxilla suture in lateral view, the last maxillary alveolus being placed at the level of the jugal-maxilla suture, and the presence of an additional pleurocoel in the first two dorsal centra vertically-aligned with the main pleurocoel.

The same combination of pneumatic features present in both *Shri* species is present in the first dorsal vertebra of *Luanchuanraptor henanensis* (Lü et al., 2007). Le

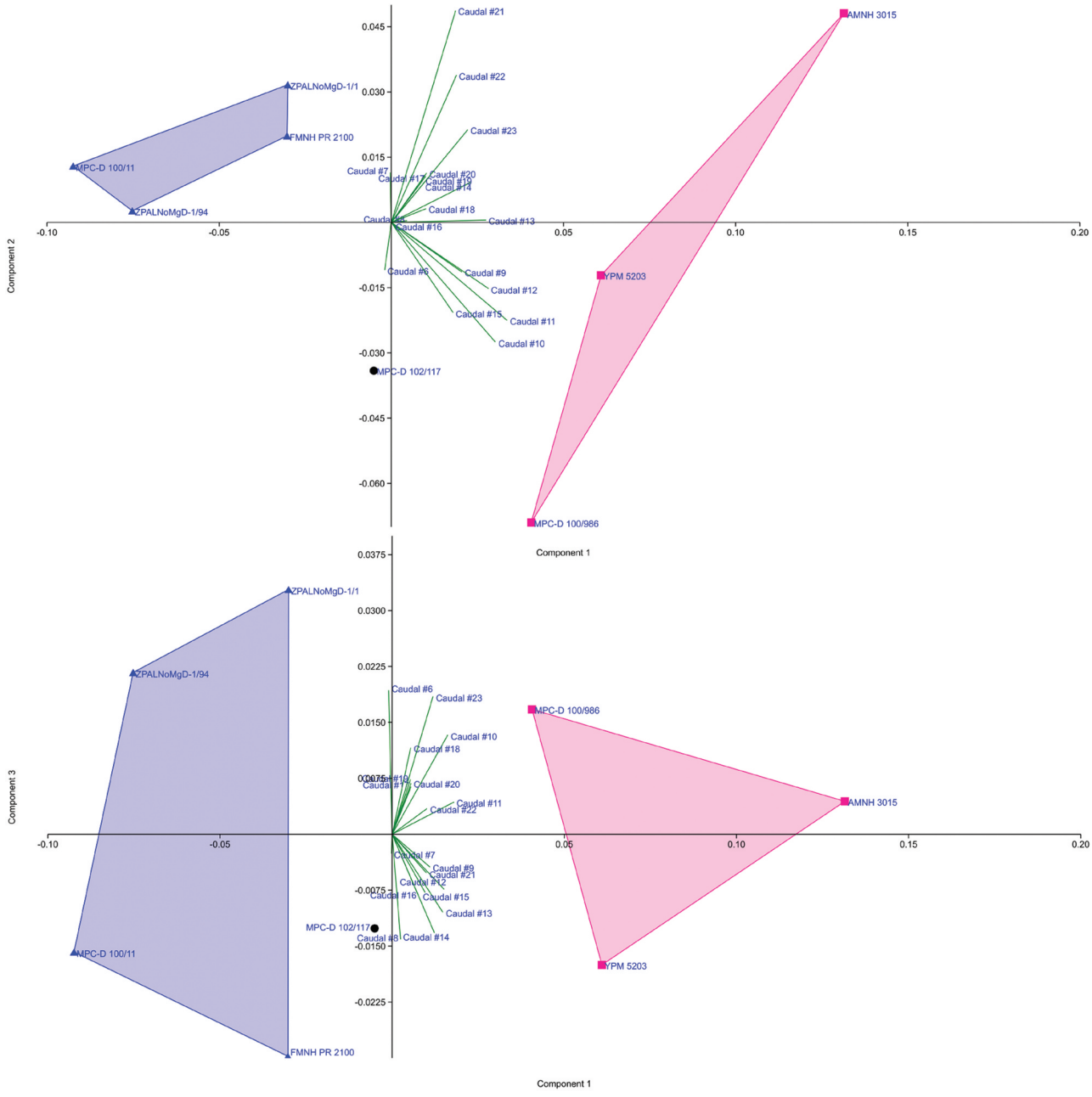

Figure 15. Diagrams of the first three components of the PCA of the caudal centra 6–23 measurements. Above, diagram of components 1 and 2. Below, diagram of components 1 and 3. Black dot, *Shri rapax*; blue triangles, non-dromaeosaurid sample; pink squares, dromaeosaurid sample. Green lines stemming from the diagram origins indicate the biplot of the caudal vertebrae ratios. Data and abbreviations in Supplementary material 1.

Loeuff & Buffetaut (1998) referred one isolated cervicodorsal vertebra from the Campanian-Maastrichtian of southern France to *Variraptor mechinorum*. The vertebra is very similar to the diagnostic cervicodorsal vertebrae of the *Shri* species in the presence of two pleurocoels aligned dorsoventrally and a deep infraprezygapophyseal fossa, but differs from the latter two taxa in the smaller size of the pleurocentral foramina, and from *Shri rapax* in bearing epipophyses. The referral of that specimen to *Variraptor* hypodigm should be considered tentative. The specimen was collected in a locality (Roques-Haute, Bouchesdu-Rhône Department) placed over 45 km from the type locality of *Variraptor mechinorum* (La Bastide Neuve, Fox-Amphoux), and no cervicodorsal vertebrae are preserved in the type material of the latter (Le Loeuff & Buffetaut, 1998). Le Loeuff & Buffetaut (1998) justified such referral on the close similarity between an isolated sacral vertebra – collected from the same locality of the cervicodorsal vertebra – and the fifth sacral vertebrae of

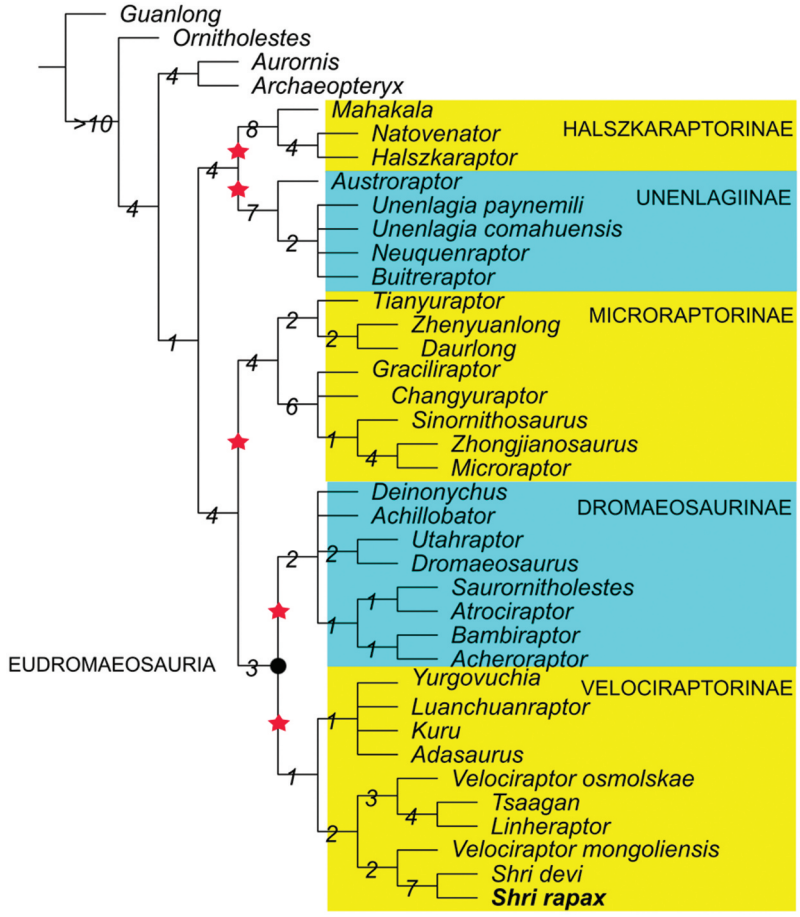

Figure 16. Strict consensus of the shortest trees found by the phylogenetic analysis. Number at nodes indicate the Bremer support. Branch-based clades indicated by the star, node-based clades indicated by the circle.

Variraptor mechinorum holotype. Yet, Le Loeuff & Buffetaut (1998) did not provide evidence of association between these two vertebrae. The features in the isolated sacral vertebra described by Le Loeuff and Buffetaut (1998) are present in the fifth sacral vertebrae of other dromaeosaurids (e.g. *Microraptor zhaoianus*, *Sinornithosaurus millenii*; Hwang et al., 2002; Xu, 2002) and cannot be considered autapomorphic of *Variraptor mechinorum*. Given the co-occurrence of two dromaeosaurid taxa in several Late Cretaceous units (Turner et al., 2012), there is no reason to assume that all dromaeosaurid material from the Campanian-Maastrichtian of Southern France belongs to *Variraptor mechinorum*. Le Loeuff and Buffetaut (1998) showed that an ilium from the type locality of *Variraptor mechinorum* likely belongs to the same individual of the type material. That ilium differs from most eumaniraptorans, including both species of *Shri*, in having the pre-acetabular process deeper and significantly longer than the postacetabular process, and in the posterodorsally concave dorsal margin of the postacetabular process: both features are widespread among early-diverging dromaeosaurids and avialans (e.g. Novas et al., 2021). Pending new evidence in support of its association, the *Variraptor* hypodigm (*sensu* Le Loeuff & Buffetaut, 1998) could include two or more taxa (i.e. a '*Shri*-like' eudromaeosaur and a non-eudromaeosaurian paravian).

The presence of autapomorphies of *Shri* in both the skull and the presacral vertebrae of MPC-D 102/117 confirms the referral of the second specimen of *Shri devi* to the latter taxon by Czepiński (2023) despite the limited anatomical overlap of those two fossils. Yet, several postcranial features differentiate the Djadokhtan *Shri rapax* from the holotype of the Baruungoyotan *Shri devi*. These include the proportions among the middle cervical centra (similarly-elongated in *Shri rapax*, showing a marked disparity of elongation in *Shri devi*), the presence of the accessory pleurocoel in the last cervical centrum (absent in *Shri devi*), the larger size of the accessory cervicodorsal pleurocoels, the more extensive pneumatization of the cervicodorsal neural arches, the absence of epipophyses in the cervicodorsal vertebrae, the different caudal inclination of the pubis, the shape and elongation of the ischium, the reduced

extent of the ischial obturator process, the absence of the ischial tuberosity, and the morphology of the lateral shelf of the ischium (Figure 17). Other differences, in particular in the shape and proportions of the iliac preacetabular blades, might be at least in part due to taphonomic artefacts. Furthermore, based on the cast of the skull, the antorbital region of *Shri rapax* seems relatively shorter and the suborbital ramus of jugal dorsoventrally more robust than in *Shri rapax*. Given the similar size of MPC-D 102/117 and both *Shri devi* specimens, most of these differences, in particular those in the postcranial skeleton, are unlikely to be ontogenetically-controlled features, and support a species-level distinction.

The morphological differences between *Shri rapax* and *Shri devi* are consistent with their suggested stratigraphic distinction. Although usually assumed as diachronous, with the former older than the latter, the stratigraphic relationships between the Djadokhtan and Baruungoyotan localities are more complex and also include lateral transitions (Jerzykiewicz et al., 2021). According to the lithobiotope concept (Jerzykiewicz et al., 2021), the faunal distinctions among these localities could not be simply interpreted as the result of phyletic (anagenetic) patterns and may also involve geographic and/or environmental vicariance between closely-related species and ecological segregation among sympatric taxa (Godefroit et al., 2008). This scenario might explain the co-occurrence in the Djadokhtan unit of three velociraptorines (*Velociraptor*, *Shri* and *Tsaagan*), two of which very closely-related (*Velociraptor* and *Shri*) yet showing the most significant disparity in snout features related to ecological adaptations (Czepiński, 2023; Powers et al., 2021).

Our phylogenetic analysis agrees with Powers et al. (2021) in reconstructing *Velociraptor* as non-monophyletic, with *Velociraptor osmolskae* closer to *Linheraptor exquisitus* and *Tsaagan mangas* than to *Velociraptor mongoliensis*, and the latter closer to the *Shri* species. Due to the fragmentary nature of the *Velociraptor osmolskae* hypodigm (Godefroit et al., 2008), the support of the clade including the latter and the '*Tsaagan - Linheraptor*' node is relatively weak. If the two *Velociraptor* species are enforced as sister taxa, the shortest trees found are only two steps longer than the shortest topologies obtained under no constraints. Accordingly, we follow Godefroit et al. (2008) and do not suggest a genus-level revision of *Velociraptor osmolskae* pending additional material referred to the latter species. An alternative taxonomic option preserving *Velociraptor* monophyly would be to lump *Linheraptor*, *Shri* and *Tsaagan* into *Velociraptor* (as, respectively, '*Ve. exquisitus*", "*Ve. devi*", "*Ve. rapax*" and "*Ve. mangas*'). Although the inclusiveness of any genus-level taxon is arbitrary, we note that the latter (lumping) taxonomy would be consistent with the restricted stratigraphic and geographic range of this cluster of species, all collected from similar units from Inner Mongolia and southern Mongolia, and the overall '*Velociraptor*-like' morphology shared by all of them (Barsbold & Osmólska, 1999; Norell et al., 2006; Powers et al., 2021). Regardless to the taxonomic system followed, assuming temporal overlap between the Djadokhta-like units, the high number of velociraptorine species co-occurring in the arid to semi-arid palaeoenvironmental context inferred from their fossiliferous facies (Dingus et al., 2008) is comparable to the co-occurrence of several species of *Varanus* in the Great Desert in modern Australia (Pianka, 1994).

The most unusual feature of *Shri rapax* is the exceptional robustness of the hand. In particular, when scaled to the same length, all elements of the pollex are approximately 150% transversely more robust than the homologous elements in other Djadokhtan dromaeosaurids (e.g. *Velociraptor mongoliensis*, Norell & Makovicky, 1999), and proportionally stouter than any other known dromaeosaurid (e.g. Ostrom, 1969; Hwang et al., 2002; Wang et al., 2022). The proximoventral tubercle of the pollex ungual in *S. rapax* is very prominent and marked by distinct rugosities, which suggest the tight anchoring of well-developed flexor muscles (Ostrom, 1969). Furthermore, the first manual ungual in MPC-D 102/117 is proportionally longer than in the other dromaeosaurids. Using the length of the humerus as a proxi of forelimb size, the anterior limb of *S. rapax* is about 64% the size of that of *Deinonychus antirrhopus* AMNH 3015 (Ostrom, 1969). Yet, despite its smaller body and forelimb size, the pollex ungual in the new Mongolian species is approximately as long as in the North American taxon (i.e. 79.5 mm *vs* 80 mm, both measured along the outer curve; Ostrom, 1969). This condition is absent in the other Mongolian dromaeosaurids: compared to the Djadokhtan velociraptorines of similar body size (e.g, MPC-D 100/982, Norell & Makovicky, 1999), the pollex ungual of MPC-D 102/117 is about twice longer (i.e. 39.9 mm *vs* 79.5 mm, both measured along the outer curve). Recent studies have concluded that prey acquisition among the eudromaeosaurs was more tied to snout morphology than to the raptorial second toe claw (Powers et al., 2021). We suggest that hand morphology also played a role in shaping the ecological preferences of the dromaeosaurids. Direct taphonomic evidence indicates that dromaeosaurids actively used the hands in predation (Carpenter, 2000): in the 'Fighting Dinosaurs' (an associated *Velociraptor mongoliensis* and *Protoceratops andrewsi* pair from the Djadokhta Formation of

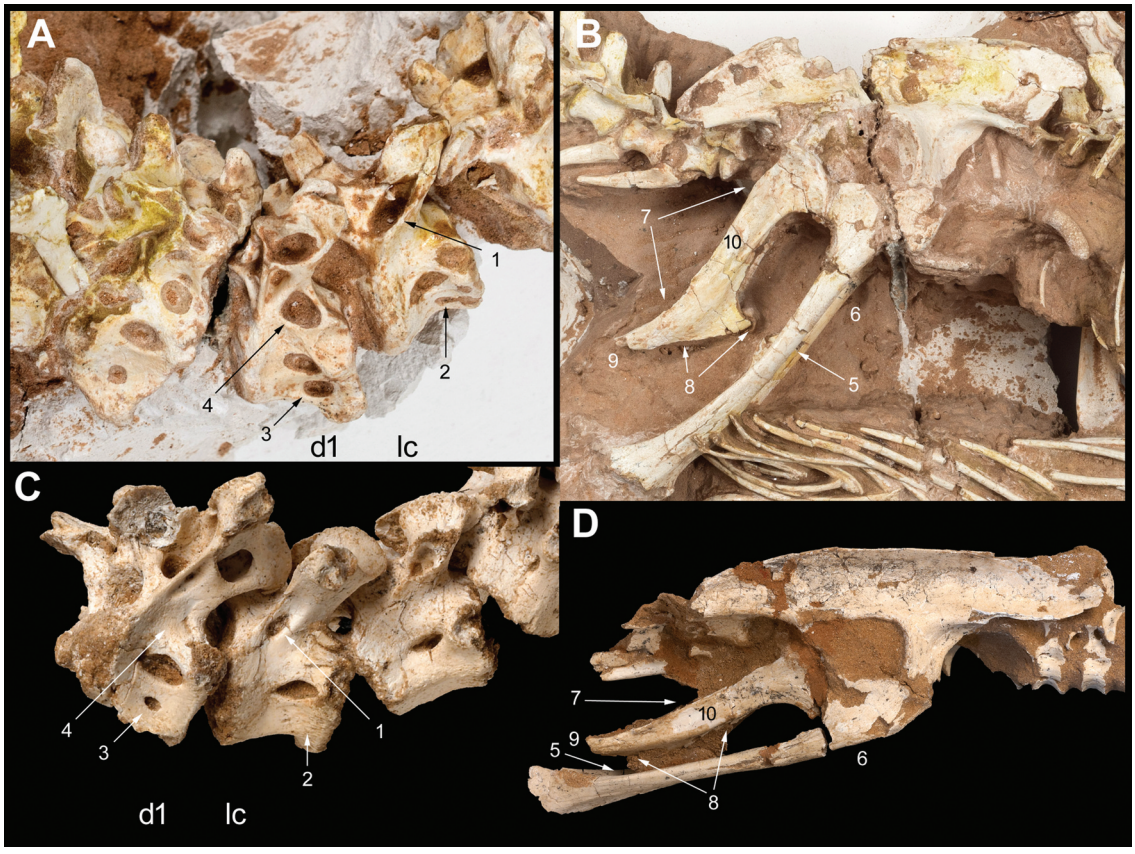

Figure 17. Selected elements of *Shri rapax* holotype MPC-D 102/117 (a, b) and *Shri devi* holotype MPC-D 100/980 (c, d). (a, c), cervicodorsal transition in right lateral view. (b, d) pelvis in lateral view (d, reversed for comparison). Features differentiating *S. rapax* from *S. devi* (condition in the latter in italics): 1, last cervical vertebra with merged infraprezygapophyseal and infradiapophyseal fossae (*distinct*); 2, last cervical centrum with accessory pleurocoel (*absent*); 3, first dorsal centrum with large accessory pleurocoel placed cranioventrally to main pleurocoel (*accessory pleurocoel small and placed ventrally*); 4, first dorsal neural arches with large accessory fossa (*fossa absent*); 5, pubis and ischium diverging distally in lateral view (*subparallel*); 6, pubis inclined 135° caudoventrally (*more than 155°*); 7, posterior margin of ischium proximally convex and distally concave (*straight*); 8, obturator process extended for half of ischium (*two-thirds of ischium*); 9, ischium as long as two-thirds of pubis (*about half of pubis*); 10, ischium with longitudinal sulcus dorsal to sharp lateral shelf and no tuber (*sulcus absent dorsal to rounded ridge and tuber present*). Abbreviations: d1, first dorsal vertebra; lc, last cervical vertebra.

Tögrögiin Shiree, Mongolia; Barsbold, 1983), the left hand of the *Velociraptor* is grasping the face of the *Protoceratops*. Furthermore, the right forearm of the same *Velociraptor* is between the clenched jaws of the *Protoceratops* (Carpenter, 2000), suggesting that the forelimbs of these predators were a preferential target by the prey during the attack. It is intriguing to note that the *Velociraptor* in this case failed the predation and succumbed along with its prey; yet even in the case that it survived, it received a severe wound on its right forearm. Additional specimens support direct ecological interactions between Djadokhtan velociraptorines and *Protoceratops*-grade ceratopsians. A protoceratopsian skull was found along side the *Velociraptor mongoliensis* holotype (Osborn, 1924). Given the peculiar taphonomic and preservational patterns of the dinosaur skeletons found in the Djadokhta fossiliferous facies (Dingus et al., 2008), we dismiss *post-mortem* transport and suggest a direct *peri-mortem* association between *Velociraptor mongoliensis* holotype and the *Protoceratops* skull mentioned by Osborn (1924). Hone et al. (2010) described shed velociraptorine teeth associated to tooth-marked bones of a protoceratopsian skeleton at Bayan Mandahu (Inner Mongolia) which confirm the recurrent ecological interaction between these taxa.

We suggest that frequent interactions with the ceratopsians (Hone et al., 2010), combined with active antipredatory behaviour by the latter (Carpenter, 2000), could had promoted the evolution of more robust forearms and stockier hands among some Djadokhtan velociraptorines. If we assume that *Shri rapax* shared the predatory behaviour of its close relative *Velociraptor mongoliensis*, the more robust proportions of its hands

imply that it was better adapted to target larger and more robust prey than those usually preyed on by *Velociraptor*. Robustly-built neoceratopsian and armoured dinosaurs (Ankylosauridae) are relatively abundant in the Djadokhta-like lithobiotopes, whereas the more gracily-built ornithopods are rare (Gilmore, 1933; Jerzykiewicz et al., 2021; Kurzanov, 1990, 1992; Maryańska & Osmólska, 1975).

Additional anatomical evidence supports niche partitioning among the Djadokhtan velociraptorines. The snout of both *Shri* species is proportionally shorter and stouter than in *Velociraptor*, the tooth row is more caudally extended, and the jugal-maxillary suture is interdigitated instead of being a simple contact (Czepiński, 2023): all these features have been considered in support of a stronger bite in *Shri* than in *Velociraptor* (Powers et al., 2021; Sakamoto, 2010; Therrien et al., 2005; Tse et al., 2024).

It is noteworthy that all above-listed features differentiating the skull of the two *Shri* species from the other velociraptorines are shared by some dromaeosaurines (e.g. *Saurornitholestes langstoni*, *Atrociraptor marshalli*; Powers et al., 2021), and could support an alternative placement of the former genus among Dromaeosauridae (see topology in Wang et al., 2022, based on a previous iteration of our phylogenetic data set). Yet, using the updated data set of our study and enforcing *Shri* genus in Dromaeosaurinae, all shortest trees found are nine steps longer than the shortest unenforced topologies: we thus agree with Czepiński (2023) that the similarities between *Shri* and some dromaeosaurines/saurornitholestines are due to convergence. This suggests that *Shri* diverged from the ecological regime(s) shared by the other Mongolian velociraptorines, eventually converging towards the more generalist and possibly even more macrophagous predatory behaviour suggested for the other eudromaeosaurs (Ostrom, 1969; Powers et al., 2021).

Other features in the postcranium further confirm this ecological scenario. The falciform second pedal ungual of *Shri devi* is hypertrophied, proportionally larger than those of all other members of Velociraptorinae (Czepiński, 2023; Turner et al., 2021). Although no feet are preserved in *Shri rapax*, the hypertrophy of the second pedal ungual of *Shri devi* (compared to other velociraptorines) recalls the comparable pattern in the first manual ungual of *Shri rapax*, and might represent an additional autapomorphy of the genus *Shri*. In predatory birds, both size and curvature of the unguals are related to the maximum size of the prey and are a good indicator of feeding ecology, niche partitioning and prey preference (Tsang et al., 2019), an approach applied to paravian theropods (Pittman et al., 2022). In summary, the hypertrophied unguals in the fore- and hindlimbs in the species of *Shri* confirm niche partitioning from the sympatric *Velociraptor mongoliensis* and possible preference for larger and more robustly-built prey items. The lines of evidence from both skull and limbs thus converge to some ecological segregation and reduced niche overlap among the sympatric dromaeosaurids found in the Djadokhtan lithobiotopes and help explaining the rich diversity of velociraptorines from the Nemegt Basin.

Conclusion

We describe a new dromaeosaurid from the Djadokhta Formation of Mongolia, and erect a new species of *Shri*, *Shri rapax*. Several features in the cranial and appendicular skeleton, all related to the predatory habit of dromaeosaurids, suggest that both species of *Shri* were adapted to handling vertebrate prey items larger than those preferred by the other Djadokhtan dromaeosaurids, potentially including the larger protoceratopsian-grade ceratopsians and the immature individuals of the armoured dinosaurs.

Acknowledgments

We thank the team of Raphus.be for their help and advice during the preparation of MPC-D 102/117, and Thierry Hubin (RBINS) for the assistance in the photography of the specimen. Łukasz Czepiński, Scott Hartman and Mickey Mortimer gave significant suggestions to a preliminary version of this manuscript. We thank the Editorial Board of Historical Biology, an anonymous reviewer, Daniel Madzia and Michael Pittman for the comments and suggestions which improved the quality of the manuscript.

Disclosure statement

No potential conflict of interest was reported by the author(s).

References

Agisoft. (2018). PhotoScan Professional Edition. https://www.agisoft.com/

Agnolín, F., & Novas, F. E. (2013). *Avian ancestors: A review of the phylogenetic relationships of the theropods Unenlagiidae, Microraptoria*, Anchiornis *and Scansoriopterygidae* (p. 96). Springer Netherlands.

Balanoff, A. M., & Norell, M. A. (2012). Osteology of *Khaan mckennai* (Oviraptorosauria: Theropoda). *Bulletin of the American Museum of Natural History*, *372*, 1–77. https://doi.org/10.1206/803.1

Barsbold, R. (1983). Carnivorous dinosaurs from the Cretaceous of Mongolia. *Transactions of the Joint Soviet-Mongolian Paleontological Expedition*, *19*, 1–117.

Barsbold, R., & Osmólska, H. (1999). The skull of *Velociraptor* (Theropoda) from the Late Cretaceous of Mongolia. *Acta Palaeontologica Polonica*, *44*, 189–219.

Botelho, J. F., Ossa-Fuentes, L., Soto-Acuña, S., Smith-Paredes, D., Nuñez León, D., Salinas-Saavedra, M., Ruiz-Flores, M., & Vargas, A. O. (2014). New developmental evidence clarifies the evolution of wrist bones in the dinosaur-bird transition. *PLOS Biology*, *12*(9), e1001957. https://doi.org/10.1371/journal.pbio.1001957

Bradley, A. B., Burch, S. H., Turner, A. H., Smith, N. D., Irmis, R. B., & Nesbitt, S. J. (2019). Sternal elements of early dinosaurs fill a critical gap in the evolution of the sternum in Avemetatarsalia (Reptilia: Archosauria). *Journal of Vertebrate Paleontology*, *39*(5) e1700992. https://doi.org/10.1080/02724634.2019.1700992

Brochu, C. R. (2003). Osteology of *Tyrannosaurus rex*: Insights from a nearly complete skeleton and high-resolution computed tomographic analysis of the skull. *Society of Vertebrate Paleontology Memoirs*, *7*, 1–138. https://doi.org/10.2307/3889334

Burnham, D. A. (2004). New information on *Bambiraptor feinbergi* (Theropoda: Dromaeosauridae) from the Late Cretaceous of Montana. In P. J. Currie, E. B. Kopplehus, M. A. Shugart, & J. L. Wright (Eds.), *Feathered dragons: Studies on the transition from dinosaurs to birds* (pp. 67–111). Indiana University Press.

Burnham, D. A., Derstler, K. L., Currie, P. J., Bakker, R. T., Zhou, Z., & Ostrom, J. H. (2000). Remarkable new birdlike dinosaur (Theropoda: Maniraptora) from the Upper Cretaceous of Montana. *Paleont. Contr*, (13), 1–14. https://doi.org/10.17161/PCNS.1808.3761

Calvo, J. O., Porfiri, J. D., Veralli, C., Novas, F. E., & Poblete, F. (2004). Phylogenetic status of *Megaraptor namunhuaiquii* Novas based on a new specimen from Neuquén, Patagonia, Argentina. *Ameghiniana*, *41*(4), 565–575.

Carpenter, K. (2000). Evidence of predatory behavior by carnivorous dinosaurs. *Gaia*, *15*, 135–144.

Carrier, D. R., & Farmer, C. G. (2000). The integration of ventilation and locomotion in archosaurs. *The American Zoologist*, *40*(1), 87–100. https://doi.org/10.1093/icb/40.1.87

Cau, A. (2018). The assembly of the avian body plan: A 160-million-year long process. *Bollettino della Società Paleontologica Italiana*, *57*(1), 1–25.

Cau, A. (2024). A unified framework for predatory dinosaur macroevolution. *Bollettino della Società Paleontologica Italiana*, *63*(1), 1–19.

Cau, A., Beyrand, V., Barsbold, R., Tsogtbaatar, K., & Godefroit, P. (2021). Unusual pectoral apparatus in a predatory dinosaur resolves avian wishbone homology. *Scientific Reports*, *11*(1), 14722. https://doi.org/10.1038/s41598-021-94285-3

Cau, A., Beyrand, V., Voeten, D. F. A. E., Fernandez, V., Tafforeau, P., Stein, K., Barsbold, R., Tsogtbaatar, K., Currie, P. J., & Godefroit, P. (2017). Synchrotron scanning reveals amphibious ecomorphology in a new clade of bird-like dinosaurs. *Nature*, *552*(7685), 395–399. https://doi.org/10.1038/nature24679

Cau, A., & Madzia, D. (2018). Redescription and affinities of *Hulsanpes perlei* (Dinosauria, Theropoda) from the Upper Cretaceous of Mongolia. *PeerJ*, *6*, e4868. https://doi.org/10.7717/peerj.4868

Choiniere, J. N., Xu, X., Clark, J. M., Forster, C. A., Guo, Y., & Han, F. (2010). A basal alvarezsauroid theropod from the early Late Jurassic of Xinjiang, China. *Science*, *327*(5965), 571–574. https://doi.org/10.1126/science.1182143

Codd, J. R., Manning, P. L., Norell, M. A., & Perry, S. F. (2008). Avian-like breathing mechanics in maniraptoran dinosaurs. *Proceedings of the Royal Society B: Biological Sciences*, *275*(1631), 157–161. https://doi.org/10.1098/rspb.2007.1233

Currie, P. J., & Evans, D. C. (2020). Cranial anatomy of new specimens of *Saurornitholestes langstoni* (Dinosauria, Theropoda, Dromaeosauridae) from the Dinosaur Park Formation (Campanian) of Alberta. *The Anatomical Record*, *303*(4), 691–715. https://doi.org/10.1002/ar.24241

Currie, P. J., & Varrichio, D. J. (2004). A new dromaeosaurid from the Horseshoe Canyon Formation (Upper Cretaceous) of Alberta, Canada. In P. J. Currie, E. B. Kopplehus, M. A. Shugart, & J. L. Wright (Eds.), *Feathered dragons: Studies on the transition from dinosaurs to birds* (p. 112). Indiana University Press.

Czepiński, Ł. (2023). Skull of a dromaeosaurid *Shri devi* from the Upper Cretaceous of the Gobi Desert suggests convergence to the North American forms. *Acta Palaeontologica Polonica*, *68*, 227–243. https://doi.org/10.4202/app.01065.2023

Dingus, L., Loope, D. B., Dashzeveg, D., Swisher, C. C., Minjin, C., Novacek, M. J., & Norell, M. A. (2008). The geology of Ukhaa Tolgod (Djadokhta Formation, Upper Cretaceous, Nemegt Basin, Mongolia). *American Museum Novitates*, *3616*(1), 1–40. https://doi.org/10.1206/442.1

Forster, C. A., O'Connor, P., Chiappe, L., & Turner, A. (2020). The osteology of the late Cretaceous paravian *Rahonavis ostromi* from Madagascar. *Palaeontologia Electronica*, 1–75. https://doi.org/10.26879/793

Forster, C. A., Sampson, S. D., Chiappe, L. M., & Krause, D. W. (1998). The theropod ancestry of birds: New evidence from the late Cretaceous of Madagascar. *Science*, *279*(5358), 1915–1919. https://doi.org/10.1126/science.279.5358.1915

Foth, C., Tischlinger, H., & Rauhut, O. W. M. (2014). New specimen of *Archaeopteryx* provides insights into the evolution of pennaceous feathers. *Nature*, *511*(7507), 79–82. https://doi.org/10.1038/nature13467

Gauthier, J. (1986). Saurischian monophyly and the origin of birds. *Memoirs of the California Academy of Sciences*, *8*, 1–55.

Gianechini, F. A., Makovicky, P. J., Apesteguía, S., & Cerda, I. (2018). Postcranial skeletal anatomy of the holotype and referred specimens of *buitreraptor gonzalezorum* Makovicky, Apesteguía and agnolín 2005 (Theropoda, Dromaeosauridae), from the late Cretaceous of Patagonia (Theropoda, Dromaeosauridae), from the late Cretaceous of Patagonia. *PeerJ*, *6*, e4558. https://doi.org/10.7717/peerj.4558

Gianechini, F. A., & Zurriaguz, V. L. (2021). Vertebral pneumaticity of the paravian theropod *Unenlagia comahuensis*, from the upper Cretaceous of Patagonia, Argentina. *Cretaceous Research*, *127*, 127. https://doi.org/10.1016/j.cretres.2021.104925

Gilmore, C. W. (1933). Two new dinosaurian reptiles from Mongolia with notes on some fragmentary specimens. *American Museum Novitates*, *679*, 1–20.

Godefroit, P., Currie, P. J., Hong, L., Yong, S. C., & Zhi-Ming, D. (2008). A new species of *Velociraptor* (Dinosauria:

Dromaeosauridae) from the Upper Cretaceous of Northern China. *Journal of Vertebrate Paleontology*, *28*(2), 432–438. https://doi.org/10.1671/0272-4634(2008)28[432:ANSOVD]2.0.CO;2

Godfrey, S. J., & Currie, P. J. (2004). A theropod (Dromaeosauridae, Dinosauria) sternal plate from the Dinosaur Park Formation (Campanian, Upper Cretaceous) of Alberta, Canada. *Feathered Dragons: Studies on the Transition from Dinosaurs to Birds*, 144–149.

Goloboff, P., & Morales, M. (2023). TNT version 1.6, with a graphical interface for MacOs and Linux, including new routines in parallel. *Cladistics*, *39*(2), 144–153. https://doi.org/10.1111/cla.12524

Hammer, Ø., Harper, D. A. T., & Ryan, P. D. (2001). PAST: Paleontological statistics software package for education and data analysis. *Palaeontologia Electonica*, *4*(1), 1–9.

Hartman, S., Mortimer, M., Wahl, W. R., Lomax, D. R., Lippincott, J., & Lovelace, D. M. (2019). A new paravian dinosaur from the Late Jurassic of North America supports a late acquisition of avian flight. *PeerJ*, *7*, e7247. https://doi.org/10.7717/peerj.7247

Hone, D., Choiniere, J., Sullivan, C., Xu, X., Pittman, M., & Tan, Q. (2010). New evidence for a trophic relationship between the dinosaurs *Velociraptor* and *Protoceratops*. *Palaeogeography, Palaeoclimatology, Palaeoecology*, *291* (3–4), 488–492. https://doi.org/10.1016/j.palaeo.2010.03.028

Hwang, S. H., Norell, M. A., Qiang, J., & Keqin, G. (2002). New specimens of *Microraptor zhaoianus* (Theropoda: Dromaeosauridae) from Northeastern China. *American Museum Novitates*, *3381*, 1–44. https://doi.org/10.1206/0003-0082(2002)381<0001:NSOMZT>2.0.CO;2

Jasinoski, S. C., Russell, A. P., & Currie, P. J. (2006). An integrative phylogenetic and extrapolatory approach to the reconstruction of dromaeosaur (Theropoda: Eumaniraptora) shoulder musculature. *Zoological Journal of the Linnean Society*, *146*(3), 301–344. https://doi.org/10.1111/j.1096-3642.2006.00200.x

Jerzykiewicz, T., Currie, P. J., Fanti, F., & Jerzy, L. (2021). Lithobiotopes of the Nemegt Gobi Basin. *Canadian Journal of Earth Sciences*, *58*(9), 829–851. https://doi.org/10.1139/cjes-2020-0148

Jodogne, S. (2018). The Orthanc ecosystem for medical imaging. *Journal of Digital Imaging*, *31*(3), 341–352. https://doi.org/10.1007/s10278-018-0082-y

Kurzanov, S. M. (1990). A new Late Cretaceous protoceratopsid genus from Mongolia. *Paleontological Journal (In Russian)*, *4*, 91–97.

Kurzanov, S. M. (1992). A giant protoceratopsid from the Upper Cretaceous of Mongolia. *Paleontological Journal (In Russian)*, *6*, 81–93.

Lee, S., Lee, Y.-N., Currie, P. J., Sissons, R., Park, J.-Y., Kim, S.-H., Barsbold, R., & Tsogtbaatar, K. (2022). A non-avian dinosaur with a streamlined body exhibits potential adaptations for swimming. *Communications Biology*, *5*(1), 1185. https://doi.org/10.1038/s42003-022-04119-9

Le Loeuff, J., & Buffetaut, E. (1998). A new dromaeosaurid theropod from the Upper Cretaceous of southern France. *Oryctos*, *1* (1), 105–112. https://doi.org/10.1144/gsjgs.155.1.0001

Li, Q., Gao, K.-Q., Meng, Q., Clarke, J. A., Shawkey, M. D., D'Alba, L., Pei, R., Ellison, M., Norell, M. A., & Vinther, J. (2012). Reconstruction of *Microraptor* and the evolution of iridescent plumage. *Science*, *335*(6073), 1215–1219. https://doi.org/10.1126/science.1213780

Lü, J.-C., Xu, L., Zhang, X.-L., Ji, Q., Jia, S.-H., Hu, W.-Y., Zhang, J.-M., & Wu, Y.-H. (2007). New dromaeosaurid dinosaur from the Late Cretaceous Qiupa Formation of Luanchuan area, western Henan, China. *Geological Bulletin of China*, *26*(7), 777–786.

Makovicky, P. J., Apesteguía, S., & Agnolín, F. L. (2005). The earliest dromaeosaurid theropod from South America. *Nature*, *437*(7061), 1007–1011. https://doi.org/10.1038/nature03996

Makovicky, P. J., & Sues, H.-D. (1998). Anatomy and phylogenetic relationships of the theropod dinosaur *Microvenator celer* from the Lower Cretaceous of Montana. *American Museum Novitates*, *3240*, 1–27.

Mallison, H., & Wings, O. (2014). Photogrammetry in Paleontology - a practical guide. *Journal of Paleontological Techniques*, *1*, 1–31.

Marsh, O. C. (1881). Principal characters of American Jurassic dinosaurs. *Part V. The American Journal of Science and Arts*, *21*(125), 417–423. https://doi.org/10.2475/ajs.s3-21.125.417

Maryańska, T., & Osmólska, H. (1975). Protoceratopsidae (Dinosauria) of Asia. *Palaeontologia Polonica*, *33*, 134–143.

Matthew, W. D., & Brown, B. (1922). The family deinodontidae, with notice of a new genus from the cretaceous of Alberta. *Bulletin of the American Museum of Natural History*, *46*, 367–385.

Maxwell, D., & Witmer, L. (1996). New material of *Deinonychus* (Dinosauria: Theropoda). *Journal of Vertebrate Paleontology*, *16*, 51A.

Mayr, G., Pohl, B., Hartman, S., & Peters, D. S. (2007). The tenth skeletal specimen of *Archaeopteryx*. *Zoological Journal of the Linnean Society*, *149*(1), 97–116. https://doi.org/10.1111/j.1096-3642.2006.00245.x

Motta, M. J., Egli, F. B., & Novas, F. E. (2018). Tail anatomy of *Buitreraptor gonzalezorum* (Theropoda, Unenlagiidae) and comparisons with other basal paravians. *Cretaceous Research*, *83*, 168–181. https://doi.org/10.1016/j.cretres.2017.09.004

Napoli, J. G., Ruebenstahl, A. A., Bhullar, B.-A. S., Turner, A. H., & Norell, M. A. (2021). A new dromaeosaurid (Dinosauria: Coelurosauria) from Khulsan, Central Mongolia. *American Museum Novitates*, *2021*(3982), 1–47. https://doi.org/10.1206/3982.1

Nesbitt, S. J., Turner, A. H., Spaulding, M., Conrad, J. L., & Norell, M. A. (2009). The theropod furcula. *Journal of Morphology*, *270*(7), 856–879. https://doi.org/10.1002/jmor.10724

Norell, M. A., Clark, J. M., Turner, A. H., Makovicky, P. J., Barsbold, R., & Rowe, T. (2006). A new dromaeosaurid theropod from Ukhaa Tolgod (Omnögov, Mongolia). *American Museum Novitates*, *3545*(1), 1–51. https://doi.org/10.1206/0003-0082(2006)3545[1:ANDTFU]2.0.CO;2

Norell, M. A., & Makovicky, P. J. (1997). Important features of the dromaeosaur skeleton: Information from a new specimen. *American Museum Novitates*, *3215*, 1–22.

Norell, M. A., & Makovicky, P. J. (1999). Important features of the dromaeosaurid skeleton II: Information from newly collected specimens of *Velociraptor mongoliensis*. *American Museum Novitates*, *3282*, 1–45.

Norell, M. A., & Makovicky, P. J. (2004). Dromaeosauridae. In D. B. Weishampel, P. Dodson, & H. Osmólska (Eds.), The Dinosauria (pp. 196–209). University of California Press.

Norell, M. A., & Xu, X. (2005). Feathered dinosaurs. *Annual Review of Earth and Planetary Sciences*, *33*(1), 277–299. https://doi.org/10.1146/annurev.earth.33.092203.122511

Novas, F. E. (2004). Avian traits in the ilium of *Unenlagia comahuensis* (Maniraptora: Avialae). In P. J. Currie & E. B. Koppelhus (Eds.), *Feathered dragons: Studies on the transition from dinosaurs to birds* (pp. 150–166).

Novas, F. E., Agnolín, F. L., Motta, M. J., & Brissón Egli, F. (2021). Osteology of *Unenlagia comahuensis* (Theropoda, Paraves, Unenlagiidae) from the Late Cretaceous of Patagonia. *The Anatomical Record*, *304*(12), 2741–2788. https://doi.org/10.1002/ar.24641

Novas, F. E., Brissón Egli, F., Agnolin, F. L., Gianechini, F. A., & Cerda, I. (2018). Postcranial osteology of a new specimen of *Buitreraptor gonzalezorum* (Theropoda, Unenlagiidae). *Cretaceous Research*, *83*, 127–167. https://doi.org/10.1016/j.cretres.2017.06.003

Novas, F. E., & Pol, D. (2005). New evidence on deinonychosaurian dinosaurs from the Late Cretaceous of Patagonia. *Nature*, *433*(7028), 858–861. https://doi.org/10.1038/nature03285

Novas, F. E., Pol, D., Canale, J. I., Porfiri, J. D., & Calvo, J. O. (2009). A bizarre Cretaceous theropod dinosaur from Patagonia and the evolution of Gondwanan dromaeosaurids. *Proceedings of the Royal Society B*, *276* (1659), 1101–1107. https://doi.org/10.1098/rspb.2008.1554

Osborn, H. F. (1924). Three new Theropoda, *Protoceratops* zone, Central Mongolia. *American Museum Novitates*, 1–12.

Osmólska, H. (1982). *Hulsanpes perlei* n. g. n. sp. (Deinonychosauria, Saurischia, Dinosauria) from the Upper Cretaceous Barun Goyot Formation of Mongolia. *Neues Jahrbuch für Geologie und Paläontologie - Monatshefte*, *1982*(7), 440–448. https://doi.org/10.1127/njgpm/1982/1982/440

Ostrom, J. H. (1969). Osteology of *Deinonychus antirrhopus*, an unusual theropod from the Lower Cretaceous of Montana. Bull. *Bulletin of the Peabody Museum of Natural History* 30 , 1–165.

Ostrom, J. H. (1974). The pectoral girdle and forelimb function of *Deinonychus* (Reptilia: Saurischia): A correction. *Bulletin of the Peabody Museum of Natural History* 165 , 1–11.

Ostrom, J. H. (1976). On a new specimen of the Lower Cretaceous theropod dinosaur *Deinonychus antirrhopus*. *Breviora*, *439*, 1–21.

Owen, R. (1842). Report on British Fossil Reptiles. In *Part II. Report of the Eleventh Meeting of the British Association for the Advancement of Science*, Plymouth (pp. 60–204). London: John Murray.

Pei, R., Li, Q., Meng, Q., Gao, K.-Q., & Norell, M. A. (2014). A new specimen of *Microraptor* (Theropoda: Dromaeosauridae) from the Lower Cretaceous of Western Liaoning, China. *American Museum Novitates*, *3821*(3821), 1–28. https://doi.org/10.1206/3821.1

Pei, R., Li, Q., Meng, Q., Norell, M. A., & Gao, K.-Q. (2017). New specimens of *Anchiornis huxleyi* (Theropoda: Paraves) from the Late Jurassic of Northeastern China. *Bulletin of the American Museum of Natural History*, *411*, 1–67. https://doi.org/10.1206/0003-0090-411.1.1

Perle, A., Norell, M. A., & Clark, J. M. (1999). A new maniraptoran theropod, *Achillobator giganticus* (Dromaeosauridae), from the Upper Cretaceous of Burkhant, Mongolia. *Contrib Dept Geol Natl Univ Mongolia*, *101*, 1–105.

Pianka, E. R. (1994). Comparative ecology of *Varanus* in the Great Victoria Desert. *Austral Ecology*, *19*(4), 395–408. https://doi.org/10.1111/j.1442-9993.1994.tb00505.x

Pittman, M., Bell, P. R., Miller, C. V., Enriquez, N. J., Wang, X., Zheng, X., Tsang, L. R., Tse, Y. T., Landes, M., & Kaye, T. G. (2022). Exceptional preservation and foot structure reveal ecological transitions and lifestyles of early theropod flyers. *Nature Communications*, *13*(1), 7684. https://doi.org/10.1038/s41467-022-35039-1

Pittman, M., O'Connor, J. M., Tse, E., Makovicky, P., Field, D. J., Ma, W. S., Turner, A. H., Norell, M. A., Pei, R., & Xu, X. (2020). The fossil record of Mesozoic and Paleocene pennaraptorans. In M. Pittman & X. Xu (Eds.), Pennaraptoran theropod dinosaurs: Past progress and new frontiers (Vol. 440, pp. 37–95). Bulletin of the American Museum of Natural History.

Powers, M. J., Fabbri, M., Doschak, M. R., Bhullar, B. S., Evans, D. C., Norell, M. A., & Currie, P. J. (2021). A new hypothesis of eudromaeosaurian evolution: CT scans assist in testing and constructing morphological characters. *Journal of Vertebrate Paleontology*, *41*(5), 5, e2010087. https://doi.org/10.1080/02724634.2021.2010087

Sakamoto, M. (2010). Jaw biomechanics and the evolution of biting performance in theropod dinosaurs. *Proceedings of the Royal Society B: Biological Sciences*, *277*(1698), 3327–3333. https://doi.org/10.1098/rspb.2010.0794

Senter, P., Barsbold, R., Britt, B. B., & Burnham, D. A. (2004). Systematics and evolution of Dromaeosauridae (Dinosauria, Theropoda). *Bull Gunma Mus Natu Hist*, *8*, 1–20.

Senter, P., Kirkland, J. I., DeBlieux, D. D., Madsen, S., Toth, N., & Dodson, P. (2012). New dromaeosaurids (Dinosauria: Theropoda) from the Lower Cretaceous of Utah, and the evolution of the dromaeosaurid tail. *PLoS One*, *7*(5), e36790. https://doi.org/10.1371/journal.pone.0036790

Sues, H.-D. (1978). A new small theropod dinosaur from the Judith River Formation (Campanian) of Alberta Canada. *Zoological Journal of the Linnean Society*, *62*(4), 381–400. https://doi.org/10.1111/j.1096-3642.1978.tb01049.x

Therrien, F., Henderson, D. M., & Ruff, C. B. (2005). Bite me. Biomechanical models of theropod mandibles and implications for feeding behavior. In K. Carpenter (Ed.), The carnivorous dinosaurs (pp. 179–237). Indiana University Press.

Tickle, P. G., Ennos, A. R., Lennox, L. E., Perry, S. F., & Codd, J. R. (2007). Functional significance of the uncinate processes in birds. *Journal of Experimental Biology*, *210*(22), 3955–3961. https://doi.org/10.1242/jeb.008953

Tsang, L. R., Wilson, L. A. B., Ledogar, J., Wroe, S., Attard, M., & Sansalone, G. (2019). Raptor talon shape and biomechanical performance are controlled by relative prey size but not by allometry. *Scientific Reports*, *9*(1), 7076. https://doi.org/10.1038/s41598-019-43654-0

Tse, Y. T., Miller, C. V., & Pittman, M. (2024). Morphological disparity and structural performance of the dromaeosaurid skull informs ecology and evolutionary history. *BMC Ecology and Evolution*, *24*(1), 39. https://doi.org/10.1186/s12862-024-02222-5

Turner, A. H., Makovicky, P. J., & Norell, M. A. (2007). Feather quill knobs in the dinosaur *Velociraptor*. *Science*, *317*(5845), 1721–1721. https://doi.org/10.1126/science.1145076

Turner, A. H., Makovicky, P. J., & Norell, M. A. (2012). A review of dromaeosaurid systematics and paravian phylogeny. *Bulletin of the American Museum of Natural History*, *371*, 1–206. https://doi.org/10.1206/748.1

Turner, A. H., Montanari, S., & Norell, M. A. (2021). A new dromaeosaurid from the late Cretaceous khulsan locality of Mongolia. *American Museum Novitates*, *2020*(3965), 1–46. https://doi.org/10.1206/3965.1

Turner, A. H., Pol, D., Clarke, J. A., Erickson, G. M., & Norell, M. A. (2007). A basal dromaeosaurid and size evolution preceding avian flight. *Science*, *317*(5843), 1378–1381. https://doi.org/10.1126/science.1144066

Turner, A. H., Pol, D., & Norell, M. A. (2011). Anatomy of *Mahakala omnogovae* (Theropoda: Dromaeosauridae), Tögrögiin Shiree, Mongolia. *American Museum Novitates*, *3722*(3722), 1–66. https://doi.org/10.1206/3722.2

Wang, X., Cau, A., Guo, B., Ma, F., Qing, G., & Liu, Y. (2022). Intestinal preservation in a birdlike dinosaur supports conservatism in digestive canal evolution among theropods. *Scientific Reports*, *12*(1), 19965. https://doi.org/10.1038/s41598-022-24602-x

Xing, X., Pittman, M., Sullivan, C., Choiniere, J., Qing-Wei, T., Clark, J., Norell, M., & Wang, S. (2015). The taxonomic status of the Late Cretaceous dromaeosaurid *Linheraptor exquisitus* and its implications for dromaeosaurid systematics. *Vertebrata Palasiatica* 53 1 , 29–62.

Xu, X. (2002). *Deinonychosaurian fossils from the Jehol Group of Western Liaoning and the coelurosaurian evolution*. Chinese Academy of Sciences.

Xu, X., Choiniere, J. N., Pittman, M., Tan, Q., Xiao, D., Li, Z., Tan, L., Clark, J. M., Norell, M. A., Hone, D. W. E., & Sullivan, C. (2010). A new dromaeosaurid (Dinosauria: Theropoda) from the Upper Cretaceous Wulansuhai Formation of Inner Mongolia, China. *Zootaxa*, *2403*, 1–9. https://doi.org/10.11646/zootaxa.2403.1.1

Xu, X., Wang, X.-L., & Wu, X.-C. (1999). A dromaeosaurid dinosaur with a filamentous integument from the Yixian Formation of China. *Nature*, *401*(6750), 262–266. https://doi.org/10.1038/45769

Xu, X., Wu, X.-C. (2001). Cranial morphology of *Sinornithosaurus millenii* Xu et al. 1999 (Dinosauria: Theropoda: Dromaeosauridae) from the Yixian Formation of Liaoning, China. *Canadian Journal of Earth Sciences*, *38*, 1739–1752.

Xu, X., Zhou, Z., & Wang, X. (2000). The smallest known non-avian theropod dinosaur. *Nature*, *408*(6813), 705–708. https://doi.org/10.1038/35047056

Xu, X., Zhou, Z., Wang, X., Kuang, X., Zhang, F., & Du, X. (2003). Four-winged dinosaurs from China. *Nature*, *421*(6921), 335–340. https://doi.org/10.1038/nature01342